THE JEJUNAL EPITHELIUM IN TRANSMISSIBLE GASTROENTERITIS OF SWINE

by

Daryl C. Thake

A Thesis Submitted to the
Graduate Faculty in Partial Fulfillment of
The Requirements for the Degree of
MASTER OF SCIENCE

Major Subject: Veterinary Pathology

Iowa State University
Ames, Iowa

1968

TABLE OF CONTENTS

INTRODUCTION

Transmissible gastroenteritis (TGE) of swine is an acute viral disease characterized by vomiting, diarrhea, dehydration, and high mortality rate in pigs under 3 weeks of age.

Previous studies of TGE have not shown significant necrotic or inflammatory changes in intestinal tissues (1, 2, 3, 4). The small intestine, especially the jejunum, is the site of the most severe lesions (1, 2, 4). In pigs under 2 weeks of age, the primary microscopic lesions include villous atrophy with decreased height of the brush border (1, 2, 4). It has been postulated that the net effect of the infection is destruction of columnar epithelium of the small intestine with temporary inhibition of normal regeneration resulting in acute malabsorption (1, 2).

The present investigation employs electron microscopy and enzyme histochemistry to define cellular changes in TGE in an attempt to gain further insight into the mechanisms involved in this and possibly other enteric diseases, especially those of viral origin.

REVIEW OF LITERATURE

Transmissible Gastroenteritis

Transmissible gastroenteritis of swine was first described in 1946 by Doyle and Hutchings (5), who described a disease characterized by vomiting, diarrhea, rapid weight loss, and high mortality rate in baby pigs. Gastritis and enteritis were the most obvious pathologic features found, with engorgement of mesenteric vessels prevalent in most cases. They reported that fluid intestinal contents, whitish or yellowish in color, were constantly found in this disease. They demonstrated the contagious nature of the disease and showed that it could be transmitted by feeding infective intestinal contents which had passed filters that normally retain bacteria.

Bay et al. (6) were able to produce TGE in pigs by oral exposure to ground tissues of the gastrointestinal tract, kidney, liver, brain, spleen and lungs from infected pigs. They were able also to produce the disease by feeding 2 cc. of a 1:100,000 dilution of ground gastrointestinal tract. Infectivity could be destroyed by exposure to 60° C. for 20 minutes or exposure to 0.5% phenol.

Feenstra et al. (7) reported gastric hemorrhage as the most significant gross lesion. The histopathologic lesions they described in the intestinal mucosa included necrotic foci, epithelial cell necrosis, hemorrhage, mucoid degeneration and infiltration by leukocytes. Whitehair et al. (8) described inflammatory changes of the mucosa and submucosa occurring primarily in the distal portion of the small intestine and to a lesser extent in the stomach and large intestine. Bay et al. (9)

found that the lesions varied with the age of the pigs. An atonic, fluid-filled intestine was their most constant gross finding in pigs that died of TGE when less than one week old. In older pigs, necrosis and more severe engorgement of vessels were present in the stomach and intestine. Histopathologic changes included gastric congestion and patchy necrosis of the epithelium, with granular and mononuclear leukocytic infiltration in the lamina propria. Small intestinal lesions were similar to those in the stomach, with more necrosis and denuding of the epithelium. They reported swollen, club-shaped villi in the small intestine. In addition, they observed nephrosis in many infected animals. The microscopic and gross lesions were more pronounced in older animals where the disease had a longer course.

Okaniwa and Maeda (10) reported that vacuole formation in the intestinal epithelium was an outstanding lesion in TGE. Destruction of the brush border, cuboidal-shaped intestinal epithelial cells and exudative changes in the lamina propria were also reported. These workers found that activation of elements of the reticuloendothelial system in lymph nodes and spleen, as well as renal degeneration, were part of the pattern of lesions observed in this study of TGE-infected pigs (11). They concluded that the most significant lesion of TGE was a serocatarrhal inflammation throughout the small intestine. On the other hand, Lee et al. (3) reported only minor intestinal changes with little cellular infiltrate and normal-appearing epithelium, and Young et al. (12) found no evidence of inflammation in experimentally infected, antibody-devoid pigs.

Villous atrophy has been reported by some as the most significant and constant lesion of TGE (1, 2, 4). Villous atrophy was most pronounced in the jejunum, ileum and, in some cases, the lower duodenum; however, the villi of the upper portion of the duodenum were usually unchanged (2, 4). A 3- to 6-fold decrease in average villous height was demonstrated in the jejunum and ileum of infected pigs, while crypt length was slightly increased (1, 2, 4). The villous-crypt ratio was found to be reduced from 7:1 in normal pigs to 1:1 in infected pigs (2, 4).

Reber and Whitehair (13) demonstrated a decreased retention of nitrogen, sodium, and potassium and depressed blood glucose levels in pigs infected with TGE. Hooper found that the net absorption of glucose was diminished in TGE-infected pigs (1).

Lee et al. (3) were unable to produce TGE by parenteral inoculation of susceptible pigs; however, they produced it in 100% of the pigs exposed orally or by contact with infected animals. They demonstrated low concentrations of virus in the blood, liver, spleen, brain and lungs and higher concentrations in the kidney and intestine during the acute phase of the illness. However, the intestine was the only site where virus persisted for several weeks following the acute phase. Viral replication has been shown to occur predominantly in the small intestine, primarily the jejunum, with no evidence of viral replication in the stomach or colon (14).

Haelterman (15) fed TGE virus to dogs and red foxes. He was able to recover the virus from the feces of the dogs for 7 days and from foxes

for 15 days following exposure. He also was able to demonstrate serum neutralizing antibodies in the dog serum and interpreted these results as evidence of viral replication within these animals.

Bay et al. (16) found that infectivity of the virus was maintained after 3 days' drying at 67-70° F. and after storage for 3 years at -28° C. The material was noninfective after treatment with 0.05% formalin. Guinea pigs, mice, rabbits and hamsters were found to be resistant to infection by this agent.

The cytopathogenicity of TGE virus in cell culture (swine kidney) first was reported by workers in Japan in 1963 (17). Okaniwa et al. (18) studied the ultrastructure of tissue culture cells infected with the Toyama strain of TGE, a cytopathic virus. They demonstrated viral particles within the tissue culture cells and found them primarily in cytoplasmic vacuoles or on the surface of the cells. The particles averaged 95 mμ in diameter.

Goodwin and Jennings (19) described field outbreaks of transmissible gastroenteritis in England. The clinical aspects reported were identical to those observed in TGE in the United States. The gross and histopathologic changes reported were similar to those reported by Bay et al. (9) and Lee et al. (3). Transmissible gastroenteritis has also been reported from Japan (20, 21), Taiwan (22), Russia (23), Germany (24) and Poland (25).

Jejunal Epithelium

The normal jejunal epithelium has been investigated extensively in several species. The general morphologic characteristics are quite

similar for all species studied. Granger and Baker (26) studied the striated border of the intestinal epithelium of rats. They described the brush border as cylindrical, perpendicular projections which averaged 0.62 μ in width. They estimated the number of microvilli per cell at 3,000 and estimated that these projections increase the absorbing surface area approximately 30 times. Zetterquist (27), however, in studying mouse jejunum, estimated that the surface area was increased approximately 14 times by the microvilli, whereas Palay and Karlin (28) estimated a 24-fold increase in surface area. They found the microvilli to vary slightly in length according to the animal and type of fixation, but their length was always nearly 1 μ and their width 0.07 μ. They were longer near the apex of the villi than at the base and were closely packed and evenly arrayed, each unit being equidistant to the 6 surrounding it. Palay and Karlin (28) also showed that each microvillus is composed of a fibrillar meshwork that merges with the filamentous terminal web just beneath the apical surface of the cell.

The columnar absorbing cells of the jejunum have interdigitations all along their lateral cell boundaries. A junctional complex occurs between adjacent epithelial cells. The junctional complex can be broken down into 3 areas (29). Nearest the apical surface, the zonula occludens encircles the entire cell, and in this area the intercellular space is obliterated. Subjacent to the zonula occludens is the zonula adherens, which also forms a continuous band around the cell. The third component of the junctional complex is the desmosome. Desmosomes may occur irregularly along the lateral cell surfaces and are not confined to the

apical region of the lateral cell membrane. They consist of plaque-like densities on opposing cell surfaces but do not form a continuous band around the cell.

The mitochondria of the supranuclear cytoplasm are primarily oriented parallel to the long axis of the cell, while those of the infranuclear cytoplasm are more irregularly arranged. Zetterquist (27) found that the Golgi apparatus of intestinal epithelium was located in close association with the nucleus in the supranuclear cytoplasm. In the vacuolar spaces of the Golgi apparatus of intestinal cells, there is a dense, granulated substance that separates the paired Golgi membranes. Zetterquist (27) described 4 other cytoplasmic components, including: (1) vesicles, (2) free granules (ribosomes), (3) homogeneous ground substance and (4) α cytoplasmic membranes (granular endoplasmic reticulum).

Palay and Karlin (28) in their study of rat intestinal villi, found that the arrangement and quantity of granular endoplasmic reticulum varied with the absorptive state of the cell. Cells that had absorbed much fat contained few granule-covered cisternae, while fasted animals had greater quantities of granular reticulum, often in ordered array (ergastoplasm of light microscopy). Palay and Karlin (28) also found large numbers of smooth-surfaced, small vesicles in the supranuclear cytoplasm beneath the terminal web.

Sibalin and Björkman (30) investigated the fine structure of porcine jejunal epithelium during the first days of life. They found that the features of porcine jejunal epithelium are similar to those

described by Palay and Karlin (28) for the rat. They also found that, in newborn pigs under fasting conditions, the intercellular spaces are undilated and only few caveolae and vesicles appeared in the supranuclear cytoplasm. However, in newborn pigs fed colostrum, a dramatic increase in vacuoles and vesicles was observed. These vesicles occurred throughout the cytoplasm. Some vacuoles were large and contained a foamy substance. The intercellular spaces in these animals were dilated and also contained a foamy substance. After 2 days of age, the numbers of vacuoles and vesicles decreased, and the intercellular spaces were narrower than in the newborn. These features remained constant for at least the first 6 weeks of life.

Crypt epithelium has several distinct morphologic characteristics that distinguish it from villous epithelium. Palade (31) described the numerous polyribosomes that are present throughout the cytoplasm of crypt cells. Trier (32) noted the presence of membrane-bounded granules, which occur only in crypt epithelial cells and to which he ascribed a secretory function (33). The microvillous border of crypt cells is shorter and more irregular than that of villous epithelium, and organelles are usually less abundant (32).

Intestinal Dynamics

The small intestinal epithelium can be divided functionally into 2 zones; the downward projections or crypts and the upward projections or villi. The crypts are primarily production zones and show no evidence of absorptive capabilities, although evidence of secretory function has been shown by Trier (33).

Leblond and Stevens (34) studied mitotic activity of the small intestinal epithelium of adult rats. They found that mitoses occurred almost exclusively in the crypts. By the use of colchicine, they estimated the average duration of mitoses to be 1.13 hours and the average time for a newly divided cell to traverse the length of the villi and be extruded at the tip to be approximately 32 hours. Lipkin et al. (35) studied the mitotic cycle and cell migration rate in human intestinal biopsy material. They injected radioactive thymidine intravenously and obtained biopsy specimens at varying time intervals following the injections. They were then able to estimate the time required for varying stages of the mitotic cycle. The migration rate or turnover rate was estimated to be about 3 days in the ileal epithelium utilizing these techniques. Quastler and Sherman (36), with similar radioactive isotope techniques, have shown that cell turnover times in the ileal epithelium of mice are slightly over 2 days. They also noted that cells actively synthesizing DNA did not appear on the villi. Their results suggest that cell differentiation may begin shortly after mitosis, but a period of about 4 hours elapses before migration of the cells can begin.

The cells move then from the crypts to the villi and up the villi to the extrusion zone at the villous tips. The turnover rate is constant in health and undoubtedly under strict control, the source of which is as yet unknown. The morphological characteristics of the villi depend on the constant renewal of the epithelium at a normal rate. Mitotic inhibition by irradiation (37) or the administration of aminopterin (38)

will result in abnormal villous shapes. Creamer (39, 40) has proposed that abnormal sizes and shapes of intestinal villi, in various conditions that create an altered luminal environment, are a result of abnormal cell dynamics and a decrease in the mature epithelial cell population.

Enzyme Histochemistry

Alkaline phosphatase has been studied more thoroughly in relation to intestinal mucosa than other enzymes. Alkaline phosphatase activity occurs predominantly in the microvilli of the intestinal epithelium (41, 42). Intensity of the reaction for alkaline phosphatase in epithelial cells varies among species (42). Esterase activity is quite variable depending on species and substrate used (42). Succinic dehydrogenase can be used as a histochemical indicator of activity of the tricarboxylic acid cycle and therefore of mitochondral activity (42). Dawson and Pryse-Davies (43) found that acid and alkaline phosphatase, succinic dehydrogenase, and esterase activity was greatest in the surface epithelium and decreased toward the base of the villi being faint or absent in the crypts. Padykula et al. (41) generally found the same to be true. They also found the reaction for ATPase greatest in surface epithelium, although staining was also present in crypt cells. Padykula et al. (41) reported reduced activity of acid phosphatase, nonspecific esterase, succinic dehydrogenase, and ATPase in humans afflicted with nontropical sprue. Alkaline phosphatase was present only in epithelial cells at the outer surface of the blunted villi in these individuals.

Maronpot and Whitehair (44) studied acid and alkaline phosphatase, succinic, and malic dehydrogenase, leucine amino peptidase, and ATPase activity in 4 control and 4 TGE-infected pigs 3 to 4 weeks of age. They found that malic and succinic dehydrogenases and acid phosphatase reactions were present in both crypt and villous epithelial cells. Alkaline phosphatase, adenosine triphosphatase and leucine amino-peptidase were active predominantly in villous epithelium. The staining reactions for all enzymes were reduced in infected animals.

METHOD OF PROCEDURE

Animals

Pigs used for experimental infections and for noninfected controls were from natural-born litters of the National Animal Disease Laboratory herd. The pigs were allowed to nurse until 3 days of age, at which time they were removed from the sows and placed in individual cages. They were maintained on a formula containing cows' milk supplemented with eggs and minerals.

Eight pigs used in this study were from 2 naturally occurring outbreaks of TGE as diagnosed clinically on the farm. Bacteria-free filtrates of intestinal contents from these animals, when inoculated into susceptible pigs, produced a clinical syndrome typical of TGE.

Experimental Inoculation

Sixteen pigs were fed 1 ml. of a bacteria-free filtrate of TGE virus (Purdue strain) containing 10^6 infective doses per ml. Six pigs were infected by contact with pigs from one of the naturally occurring outbreaks. Bacteria-free filtrates of intestinal material from both groups of pigs produced a syndrome typical of transmissible gastro-enteritis.

Preparation of Tissues

All pigs were killed by stunning and exsanguination. Six pigs used as noninfected controls were killed at 4 days of age. The pigs obtained from naturally infected herds and those exposed by contact were killed at 24-48 hours after the appearance of diarrhea and/or vomiting. Pigs

fed infective material were killed 4 each at time intervals of 24, 44, 66, and 96 hours after administration of the virus.

The viscera were exposed immediately, sections of the jejunum were tied off and small amounts of 2.5% glutaraldehyde were injected. The segments of jejunum were removed immediately and immersed in 2.5% glutaraldehyde for use in electron microscopy. They were fixed for several hours in glutaraldehyde, cut in 1 mm. square pieces and washed in phosphate-buffered saline overnight. Post-fixation in 1% osmium tetroxide was carried out for 45 minutes. The tissues were again washed in phosphate-buffered saline and dehydrated in graded alcohols of 30, 50, 70, 90, 95, and 100%. The tissues were embedded in Epon 812.®

Sections 1 μ thick were cut for orientation with phase microscopy. Thin sections were cut with a diamond knife on an LKB Ultrotome, stained with uranyl acetate and lead citrate and examined on a Philips 200 electron microscope. Tissues for light microscopy were fixed in 10% buffered formalin. Tissues examined histologically include: stomach, duodenum, jejunum, ileum, cecum, colon, mesenteric lymph node, adrenal gland, kidney, liver, spleen, pancreas, bladder and lung. Harris' hematoxylin and eosin was used to stain the tissues.

Enzyme Histochemistry

Eight infected and 4 control animals were used for enzyme histochemistry. The infected pigs were killed 48 hours after oral inoculation. Sections of jejunum were immediately immersed in a mixture of dry ice and 95% ethanol (-70° C.). Sectioning was carried out in a cryostat.

All reactions were performed on unfixed frozen tissues. The following methods were employed for enzyme localization:

1. Alkaline phosphatase - The reaction was carried out at pH 9.4 using the modified Gomori technique (45).
2. ATPase - Localization of ATPase was also carried out at pH 9.4 after the method of Padykula and Herman (46).
3. Succinic dehydrogenase - The method of Nachlas et al. was used for this reaction utilizing Nitro BT as the tetrozolium salt (47).
4. Acid phosphatase - The localization of acid phosphatase employed Bergmeyer's lead nitrate technique (48).
5. Nonspecific esterase - The naphthol-AS-acetate method as described by Pearse was used to detect esterase activity. The diazonium salt used was Fast Blue BB (45).

Control solutions were used for each enzyme reaction. The control solutions for alkaline and acid phosphatase reactions were composed of all ingredients except sodium β-glycerophosphate. For the succinic dehydrogenase reaction, the Nitro BT salt was omitted. Naphthol-AS-acetate was omitted from the solution in the esterase control. Adenosine triphosphate was excluded in the control solution for ATPase. All solutions were fresh and mixed immediately prior to their use. Samples from control and infected pigs were incubated in the same solutions. All enzyme reactions were conducted twice on the same tissues in order to confirm the results.

Fluorescent Antibody

Fluorescent antibody studies were conducted to localize the viral antigens in the intestinal tissues. Serum from swine hyperimmunized with TGE virus (Purdue strain) was used for fluorescent antibody procedures. Globulins were precipitated with ammonium sulfate and conjugated with fluorescein isothiocyanate after the method of Coons (49).

Sections of jejunum were placed in test tubes, frozen, stored at -50° C. and sectioned in a cryostat. Three controls were used: (1) noninfected pigs, (2) normal sow serum and (3) nonconjugated immune globulins for tissue absorption prior to application of conjugated globulins.

RESULTS

The severity of lesions was directly proportional to the degree of clinical signs present at time of death. Signs and lesions were pronounced in most pigs 24 hours postinoculation and remained consistent throughout the period studied.

Histopathology

The duodenum, jejunum and ileum were the most extensively involved portions of the gastrointestinal tract. The principal changes occurred in the villi (Figs. 1, 2, 4). Atrophy or decreased length of the villi was present in all infected animals, together with a decrease in the number of villi present. The villi were flattened and club shaped, especially in the jejunum and ileum (Figs. 1, 4). Fusing of the villi was prominent (Fig. 4). Villous epithelial cells in many sections were cuboidal rather than columnar in shape and the brush border was shortened.

The crypt layer was increased in thickness and appeared more cellular in infected as compared to noninfected pigs (Figs. 1, 2, 4). This, together with the decreased height and number of villi, resulted in a decreased ratio of villous epithelium to crypt epithelium, which was apparent to a varying extent in all animals.

Mitoses were increased in the crypt layer of the jejunum and ileum of infected pigs. Mitotic figures were also visible in the surface epithelium of these animals.

There were congestion and mild infiltration of the lamina propria with mononuclear cells and granular leukocytes. Vacuolation of the surface epithelium occurred in some animals, being most extensive toward

the villous tips. Partial denuding of villous epithelium was seen in 2 of the experimentally infected animals. Submucosal edema was present throughout the small intestine. Cytoplasmic basophilia, a characteristic of crypt epithelium, was retained in the villous epithelial cells of infected pigs.

These changes were most prevalent in the jejunum and ileum. The jejunum was consistently most severely involved, but in many cases the severity of the ileal lesions approached those of the jejunum (Figs. 1, 4). The duodenum was less extensively affected. Most sections of duodenum showed only a moderate decrease in the height of the villi with some decrease in their numbers. Tissues from the mid-portion of the duodenum from several animals had little or no distinguishable change.

The gastric and large intestinal mucosae were not significantly altered, although marked distention with fluid and gas was observed grossly. Focal submucosal gastric hemorrhages were present in several animals[1] (Fig. 6). No other abnormalities were seen in these sections.

A small perforation occurred in the cecum of an experimentally-infected animal (Fig. 5). There was a focal suppurative typhlitis and peritonitis in the region of the rupture. Suppuration within the cecum

---

[1]The hemorrhage may have been due to mechanical factors such as overdistention of the stomach with subsequent rupture of small capillaries as has been suggested previously (2).

was confined to the muscular layer, while the mucosa appeared normal. A thin fibrinous cast had formed over the peritoneum, closing the perforation. The perforation possibly resulted from overdistention and weakening of the cecal wall.

Lesions in Other Organs

Lesions in other organs were inconsistent. Pulmonary congestion was seen in one animal. Multiple foci of hepatic lymphoid aggregates occurred in 2 animals. Foci of extramedullary hematopoiesis were present in liver and spleen of all animals, including controls. Tubular dilatation and mild nephrosis occurred in 2 animals killed 48 hours after inoculation (Fig. 3).

Fluorescent Antibody

Fluorescent antibody studies showed that the viral antigens were located primarily in the villous epithelium, with only slight fluorescence visible in a few scattered cells of the crypt epithelium (Fig. 7). Specific fluorescence was diffuse throughout the cytoplasm of the villous, epithelial cells, and none was seen within the nuclei.

Ultrastructure

Noninfected pigs

The structure of jejunal villous epithelium in the noninfected controls used in this study corresponds to that described earlier for young pigs by Sibalin and Björkman (30). The microvilli were long and regular and covered with a thin filamentous material, probably representing glycocalyx (Figs. 8, 9). Beneath the microvillous border was a narrow

Fig. 1. Jejunum from an experimentally-infected pig with atrophy and fusing of the villi and increased depth of the crypt layer. H & E, X 150.

Fig. 2. Jejunum from a noninfected pig. H & E, X 150.

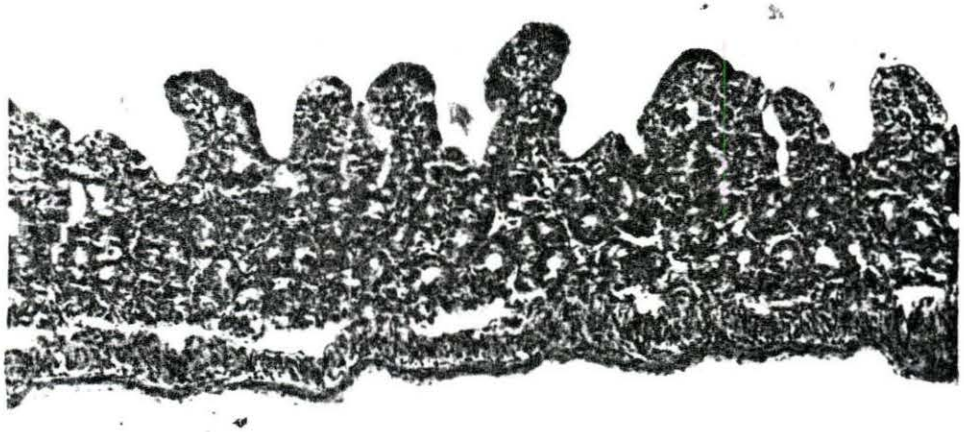

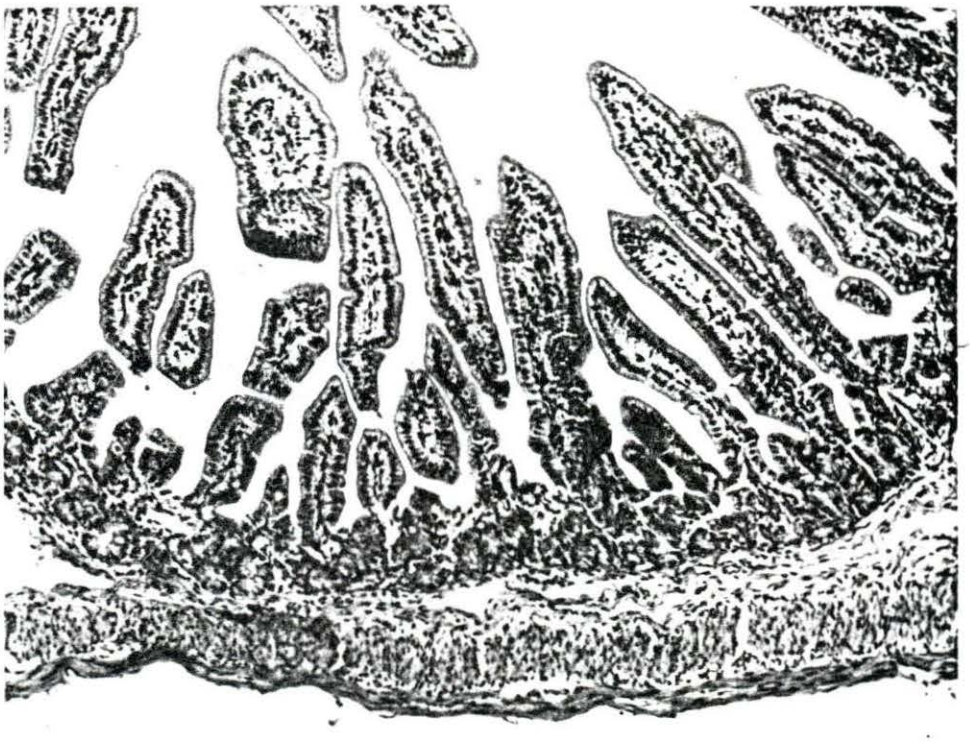

Fig. 3. Nephrosis in an experimentally infected animal with tubular dilatation and sloughing of cells into the tubules. H & E, X 150.

Fig. 4. Section from the mid-ileal region showing atrophy and fusing of the villi with vacuolation of the cells near the villous tips. H & E, X 150.

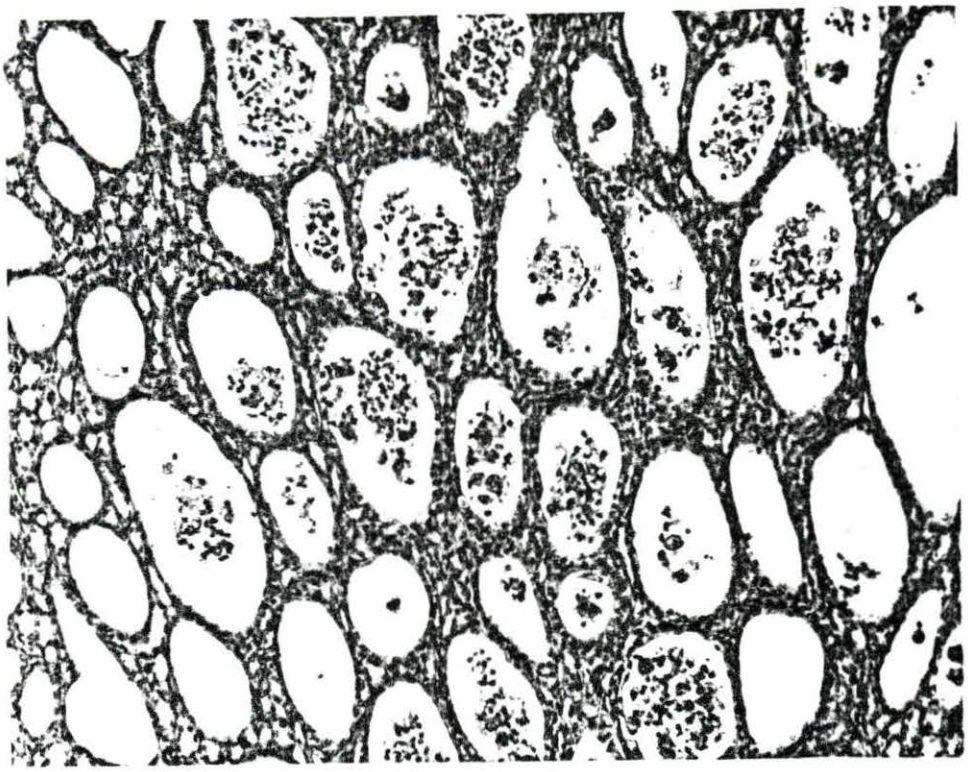

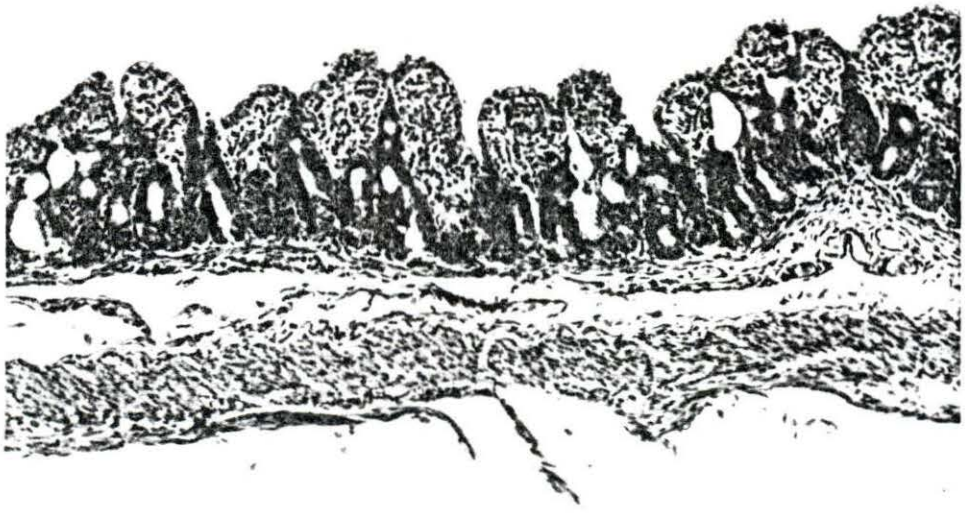

Fig. 5. Perforation through the cecal wall of an experimentally-infected pig. H & E, X 40.

Fig. 6. Submucosal gastric hemorrhage in an experimentally-infected pig. H & E, X 60.

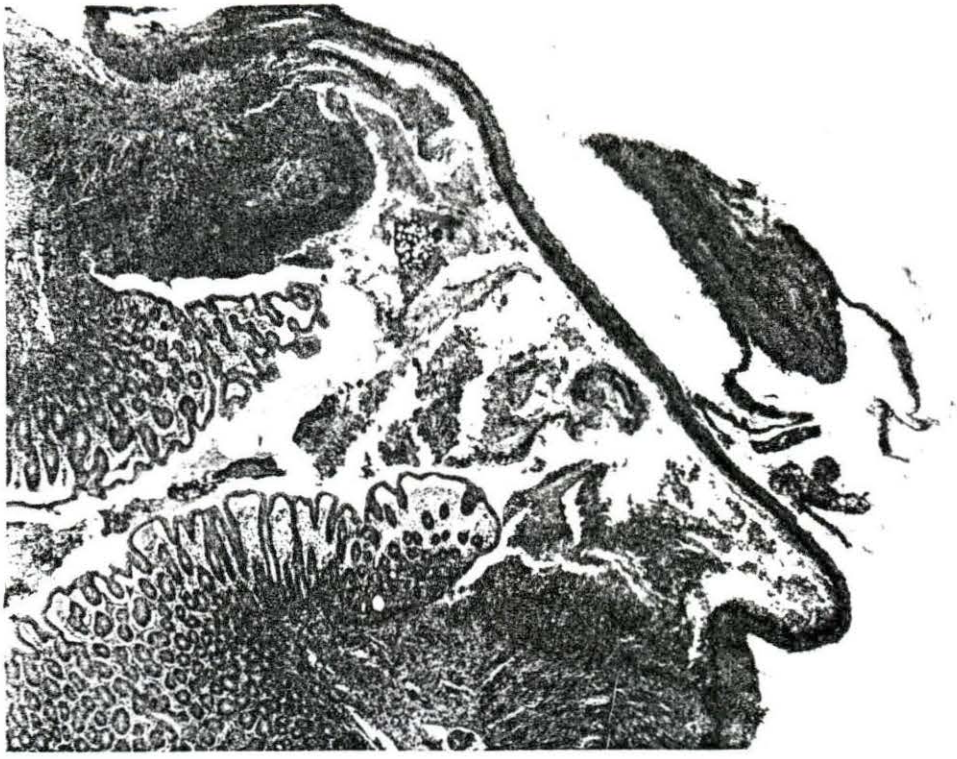

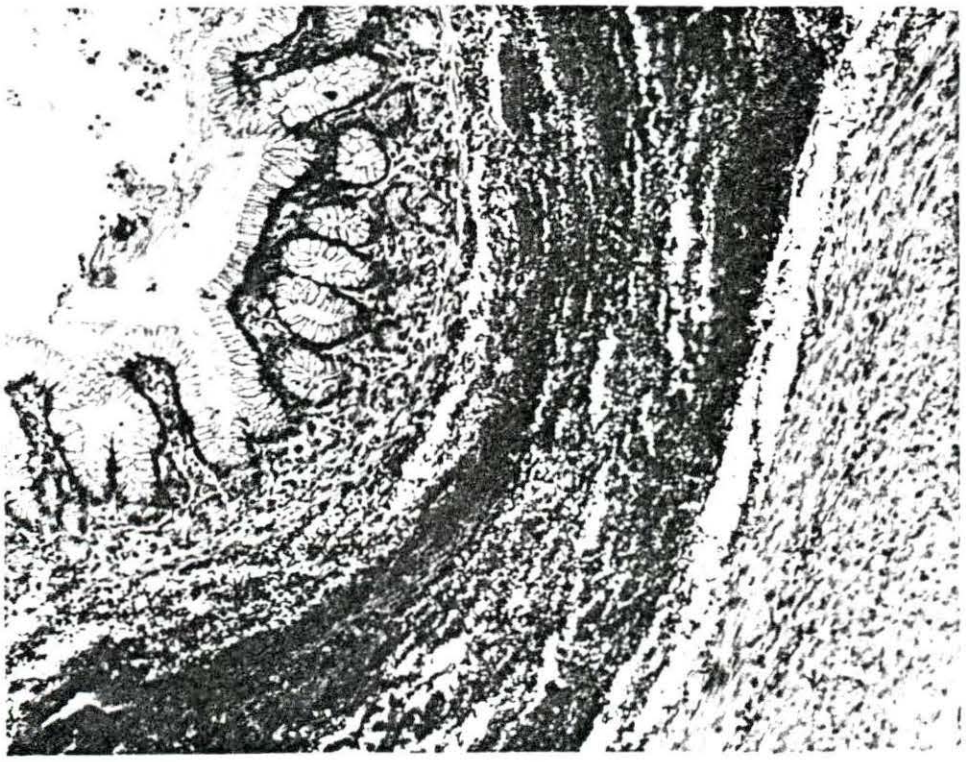

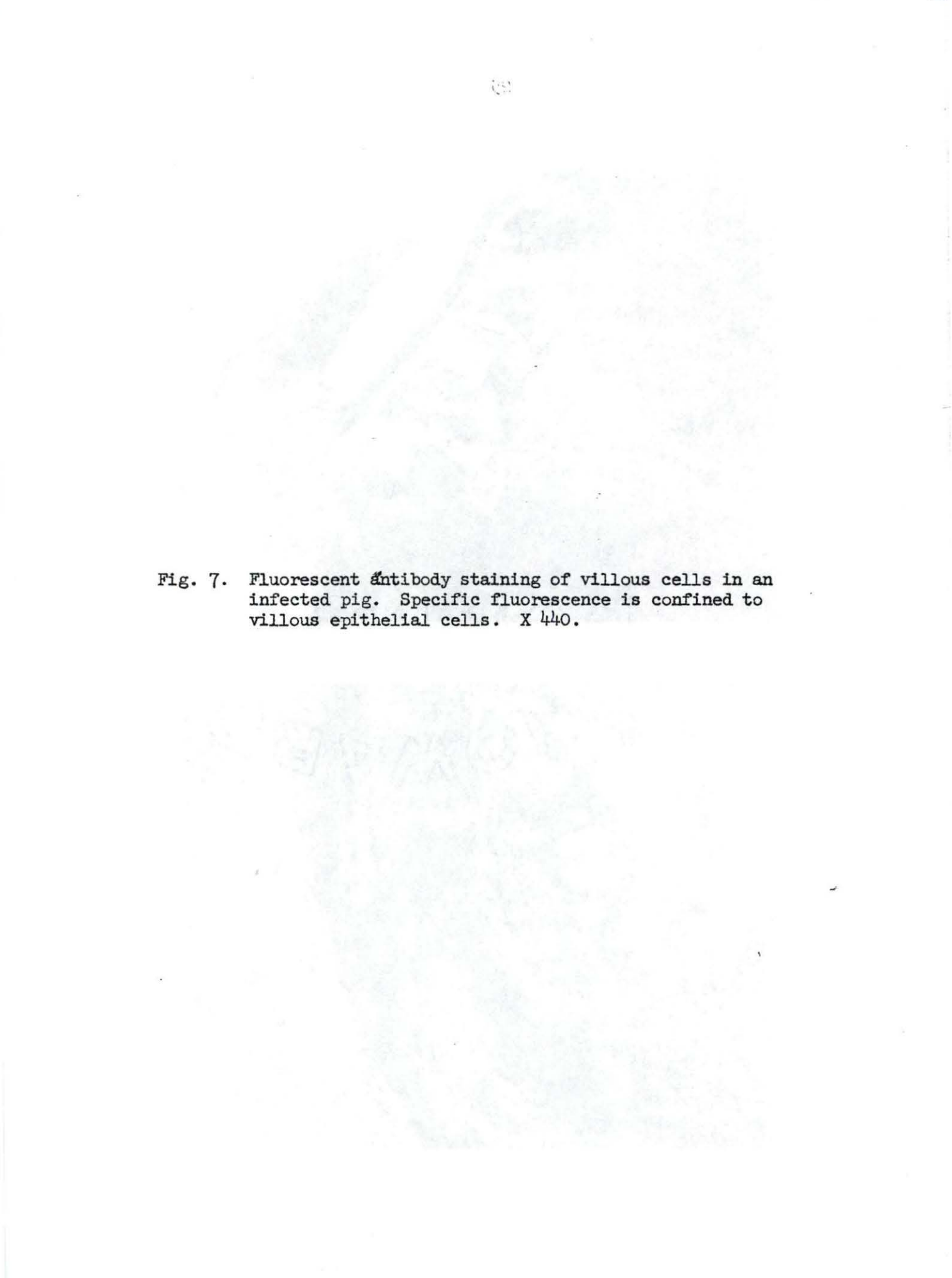

Fig. 7. Fluorescent antibody staining of villous cells in an infected pig. Specific fluorescence is confined to villous epithelial cells. X 440.

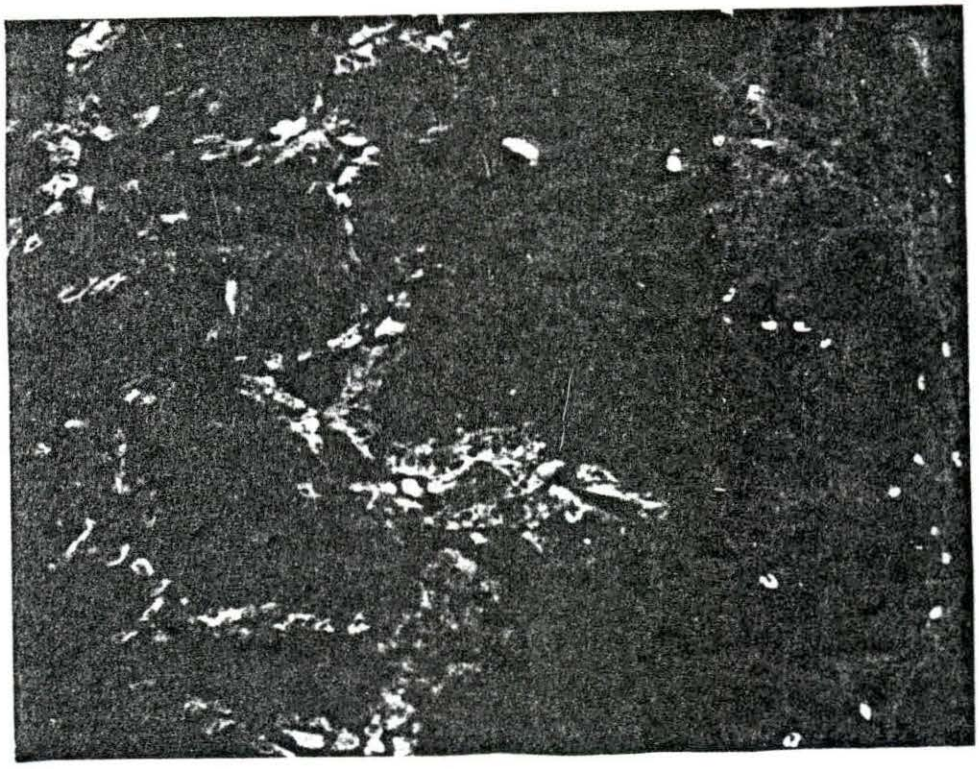

portion of cytoplasm with greater electron density and devoid of organelles. This area, the terminal web, was composed of transverse filaments into which the filaments of the microvilli inserted. Caveolae were visible at the base of the microvilli and smooth surfaced vesicles were prevalent beneath the terminal web (Figs. 8, 9). These were interpreted as evidence of pinocytosis. Deeper in the cytoplasm, the vesicles became larger and some contained an electron-dense material, probably products absorbed from the lumen of the intestine (Figs. 8, 9). The lateral borders of the epithelial cells contained numerous interdigitations with adjacent cells (Figs. 8, 9). The intercellular spaces were dilated in some areas and contained a foamy substance (Fig. 9). The mitochondria were numerous and primarily oriented in a plane perpendicular to the cell surface, especially those in the supranuclear cytoplasm. Granular endoplasmic reticulum was present and some free ribosomes were scattered throughout the cytoplasm.

Cells of the crypt epithelium possessed a number of characteristics distinctly different from villous cells. Microvilli of the crypt cells were short and irregular in spacing and arrangement (Fig. 10). Transverse filaments of the terminal web were poorly developed. No caveolae or smooth-surfaced vesicles were present in the apical cytoplasm of the crypt cells. However, membrane-bounded granules were abundant in the cytoplasm beneath the terminal web (Fig. 10). Organelles were less abundant than in villous cells, but free polyribosomes filled the cytoplasm (Fig. 10). Multivesicular bodies were common in the apical cytoplasm.

Paneth's cells[1] and argentaffin cells were not seen in the sections examined in this study. Goblet cells occurred throughout the crypt and villous epithelium (Fig. 9) and contained varying amounts of mucous granules, which were present in the supranuclear cytoplasm. Nuclei were displaced to the base of the cells containing many mucous granules. Cytoplasm of the goblet cells was dense and the granular endoplasmic reticulum was well developed.

Infected pigs

Viral particles were seen in thin sections from nearly all infected pigs. In the jejunum, the particles were seen along the surface and in the cytoplasm of the villous epithelial cells, with few visible in the crypts (Fig. 13). Similar particles were observed in swine testis tissue culture cells infected with this virus (Figs. 11, 12). The viral particles consisted of a central core measuring 40 mμ average diameter. Surrounding the central core was a narrow band of greater electron density, which in turn was surrounded by a less dense capsule with a limiting membrane (Fig. 12). The particles were 85-90 mμ average diameter. Single membrane-bounded, lysosome-like structures containing many electron-dense particles, measuring 35 mμ average diameter, were present in the cytoplasm of most infected tissue culture cells, but were not as prevalent in the infected jejunal cells (Fig. 11). These areas, which may represent

---

[1]The absence of Paneth's cells in the intestines of swine has been reported (50). Sloss (51) however, found that they were present in the jejunum primarily, also in duodenum and ileum.

sites of incomplete virus aggregations, also contained more completely formed particles consisting of all but the outer capsule. Mature viral particles in membrane-bounded cytoplasmic vacuoles were commonly seen in both tissue culture and jejunal epithelial cells. These particles appeared similar to those described by Okaniwa et al. (18).

The villous epithelium of infected pigs was altered in structure, however the crypt epithelium was similar to that of control animals (Fig. 15). The microvilli of the villous cells were short and sparse in number, with an irregular arrangement (Figs. 16, 17, 18). The microvillous border was nearly absent in some specimens (Fig. 18), while others were only moderately altered (Fig. 17). Pinocytotic vesicles, that were consistently present in villous cells of non-infected pigs, were absent from the villous epithelium of infected pigs (Figs. 16, 17, 18). There were no dilatations of the intercellular spaces. The junctional complexes and interdigitations of the lateral cell membranes remained intact. Organelles were less abundant in these cells than in normal villous epithelium. Polyribosomes, however, were very abundant, occupying most of the cytoplasm as in the cells of crypt epithelium (Figs. 16, 17, 18). The basic structural features of the villous cells of infected animals, then, were very similar to those of normal crypt epithelium. The membrane-bounded granules which are characteristic of crypt epithelium (32) were not present in the villous cells however.

Fat globules were present in many epithelial cells of the villi (Figs. 14, 16, 17, 18). Some were very large, reaching a diameter of several microns (Fig. 14). In some specimens, the fat globules

displaced most of the cytoplasm in cells located toward the villous tips (Fig. 14). The fat was often extracted during processing, leaving only a space in the cytoplasm containing a network of filamentous material (Fig. 16).

The changes in cellular organelles were inconsistent. Swollen mitochondria were present in some sections. Granular endoplasmic reticulum from a naturally infected animal was markedly distended. Changes such as these, when inconsistent, are difficult to evaluate and to distinguish from processing artifact.

Annulate lamellae were observed in tissues from both naturally and experimentally infected animals. They appeared as groups of annular formations in a regular array (Figs. 15, 19, 20). The structural characteristics of the annuli appeared identical to those of nuclear pores (Fig. 20). They were about 110 mμ average diameter. There was an electron dense spot in the center of each annulus like those seen in nuclear pores (Fig. 20). The stacked lamellar units typical of annulate lamellae were not seen, however. The groups of annuli were oriented, usually in the infranuclear cytoplasm close to the nucleus. They were often seen in close association with elements of the granular endoplasmic reticulum (Fig. 19). The annulate lamellae were present in both the crypt and villous epithelial cells of infected animals, but were not seen in noninfected animals.

Enzyme Histochemistry

The reactivity of all 5 enzymes; i.e., ATPase, acid and alkaline phosphatases, succinic dehydrogenase and nonspecific esterase, as

Fig. 8. Jejunal villous epithelium from a noninfected 4-day-old pig. Microvilli are long and regular and pinocytotic vesicles are numerous beneath the terminal web. The electron-dense material within the cytoplasm (arrows) probably represents products of absorption. X 3,400.

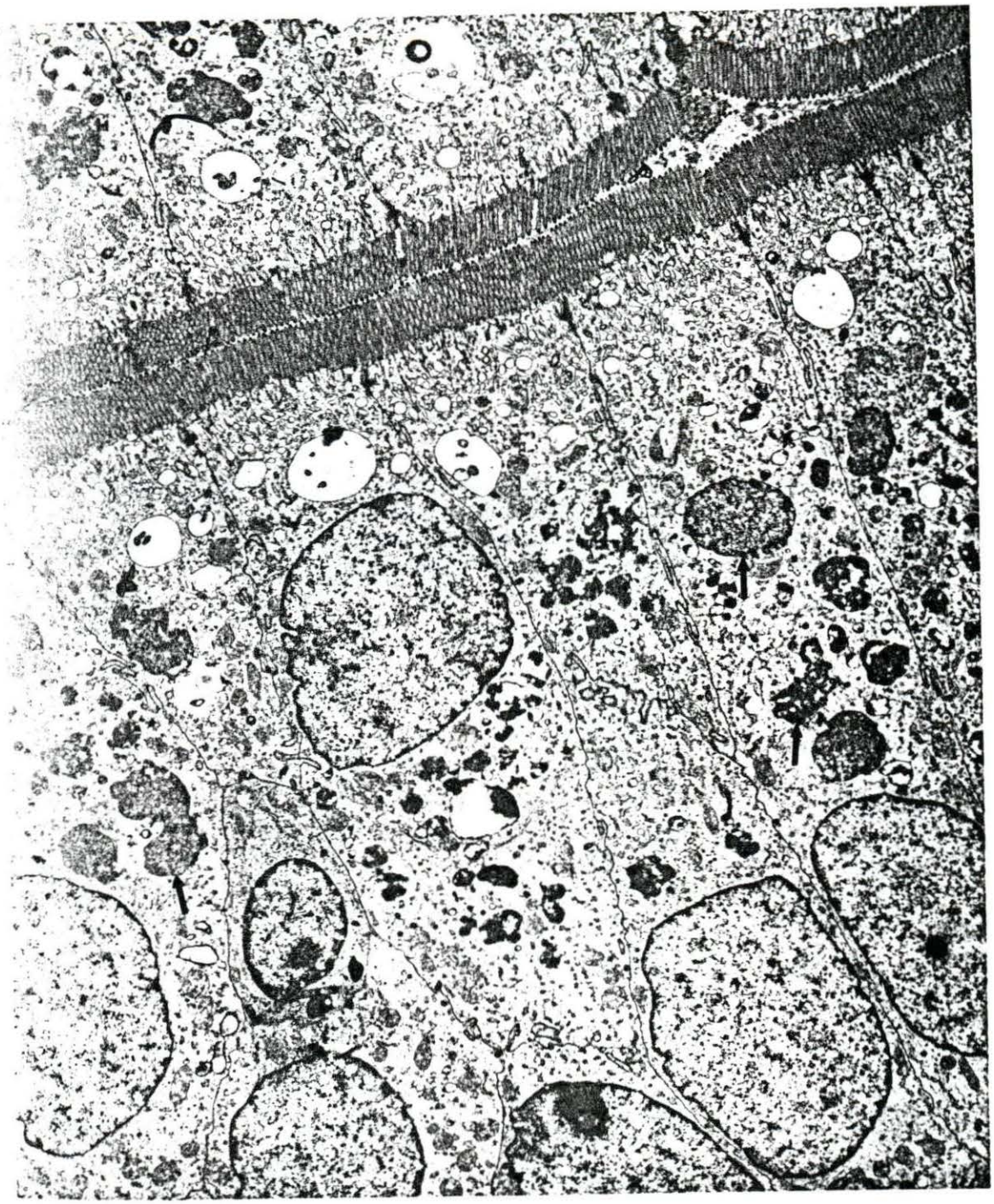

Fig. 9. Jejunal villous epithelium from a noninfected control. A goblet cell is present in this section (arrow). Dilatations of the intercellular spaces are visible, some of which contain a foamy substance. X 4,800.

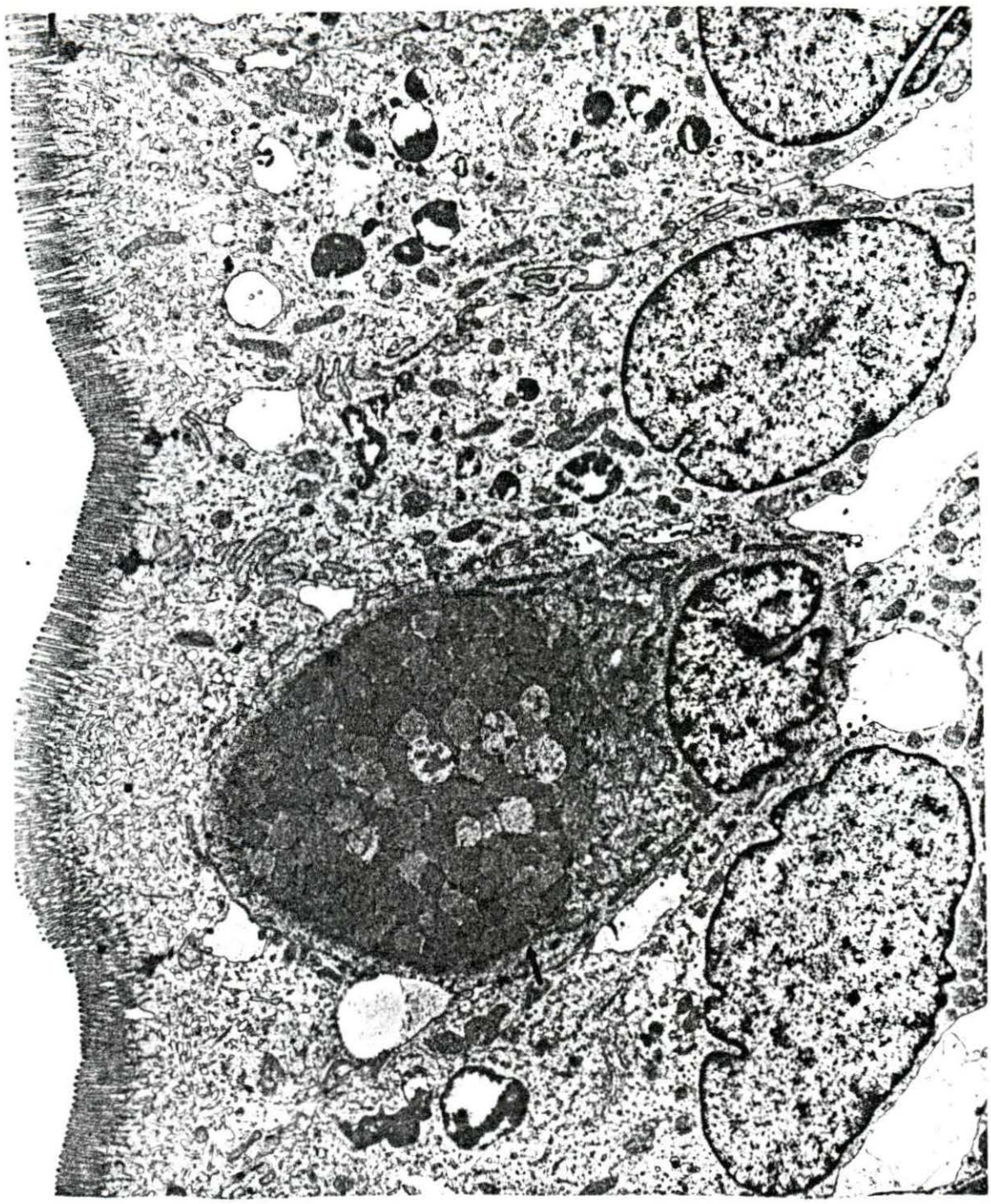

Fig. 10. Cells from the base of a crypt in a noninfected pig. The microvillous border is short and irregular. The cytoplasm is filled with polyribosomes. The membrane-bounded granules in the apical cytoplasm are characteristic of crypt epithelium. There is a migrating leukocyte near the bottom of the micrograph (arrow). X 11,000.

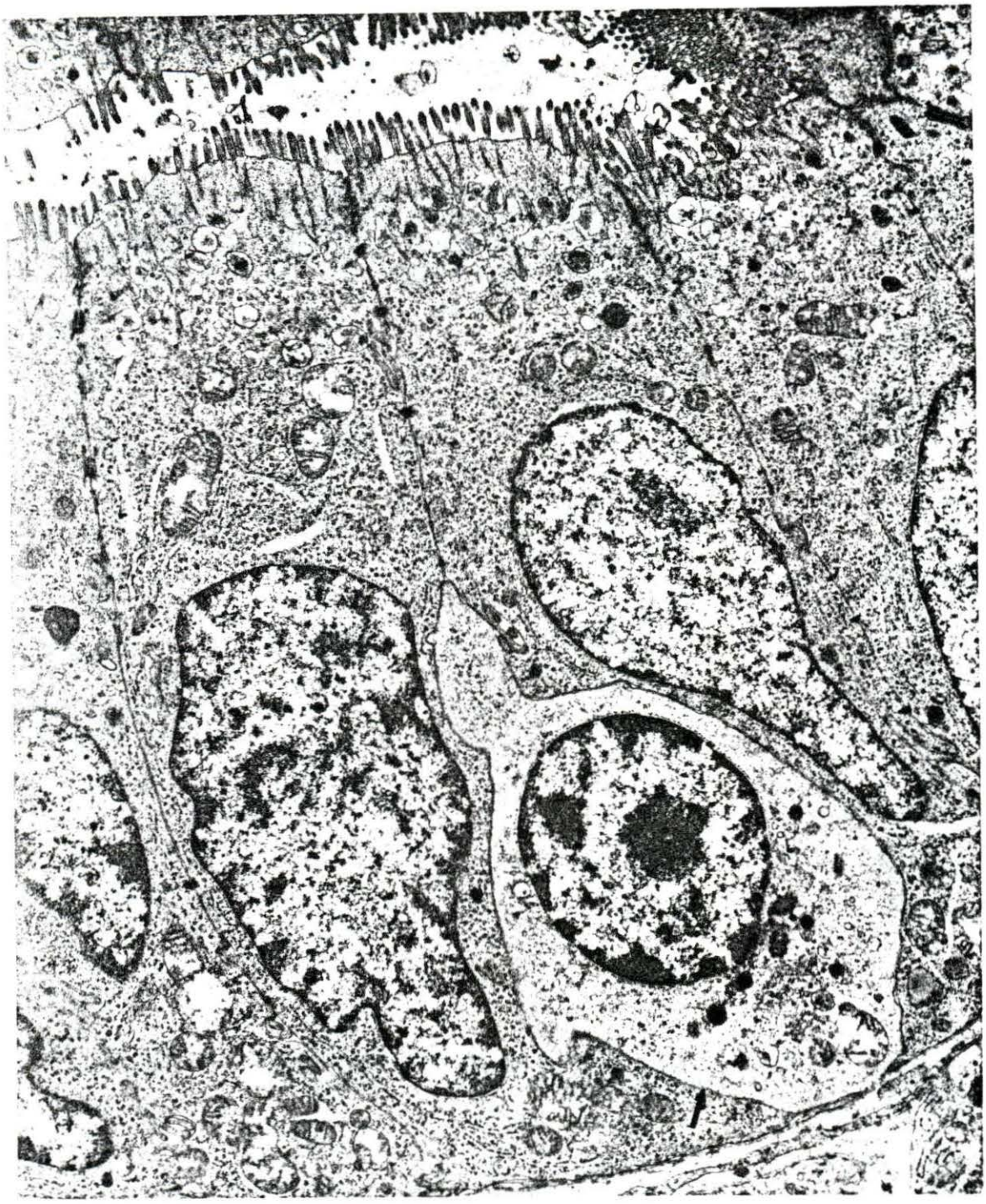

Fig. 11. Infected swine testis tissue culture cell showing aggregations of incomplete virus within single membrane-bounded, lysosome-like structures. Some contain more completely formed viral particles. X 20,000.

Fig. 12. Mature viral particles at the surface of a swine testis tissue culture cell. X 66,000.

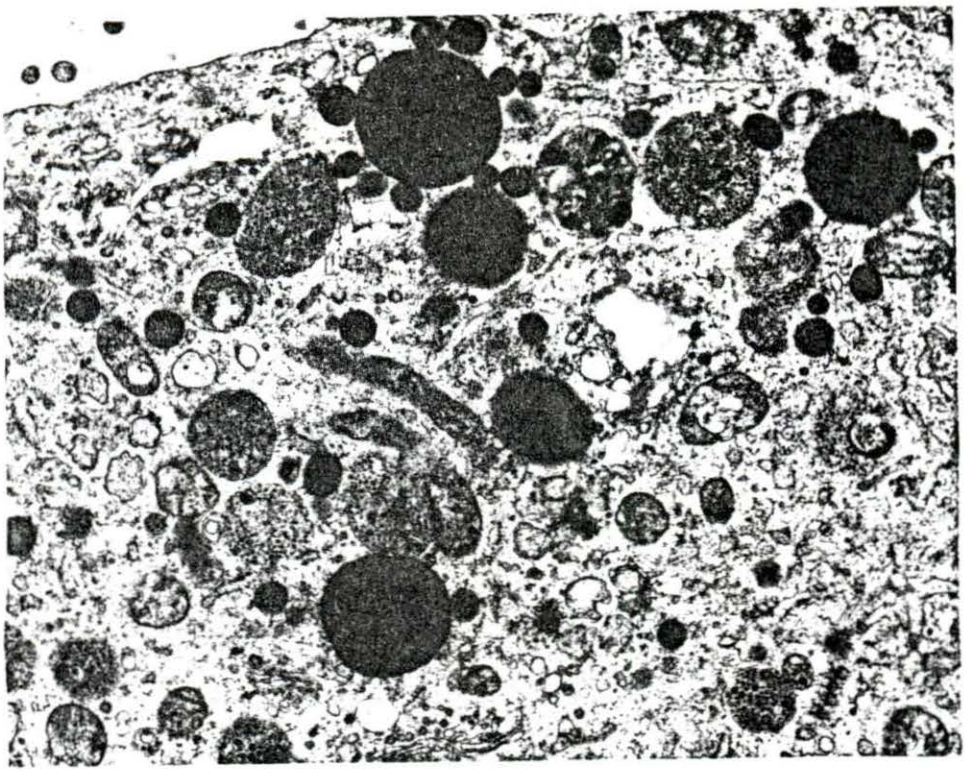

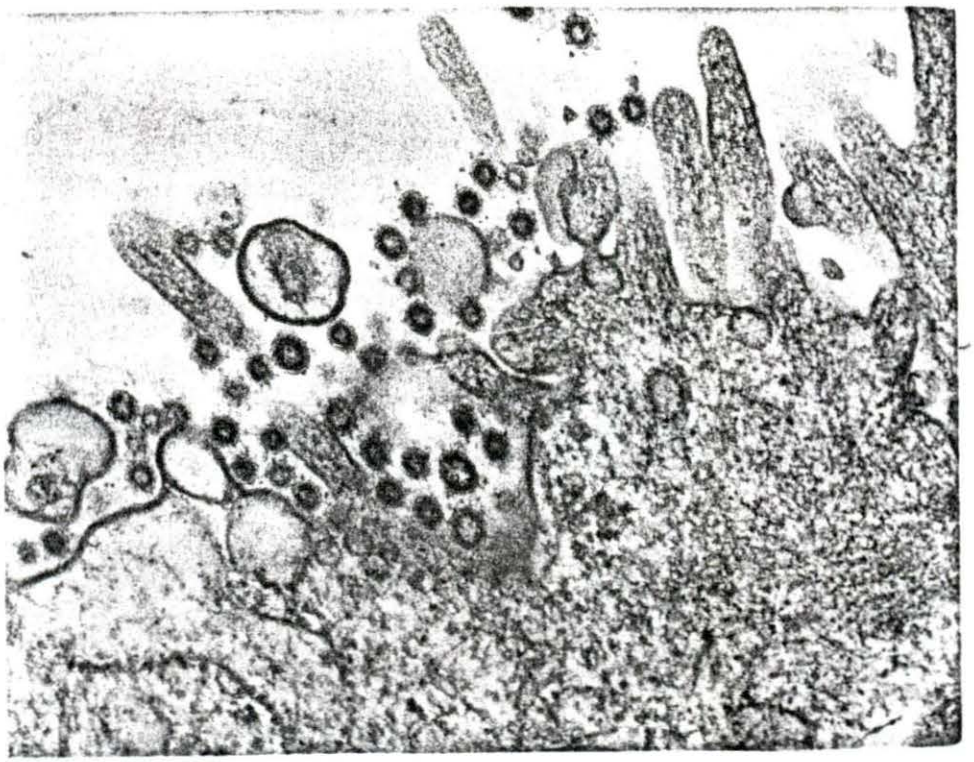

Fig. 13. Viral particles interspersed among the microvilli of a villous cell from an infected pig. Note the glycocalyx on the surface of the microvilli and insertion of the filaments of the microvilli into the terminal web, both of which appear normal in this case. X 46,000.

Fig. 14. Cell near a villous tip in an experimentally infected pig. Fat displaced much of the cytoplasm with some fat droplets measuring several microns in diameter. X 7,200.

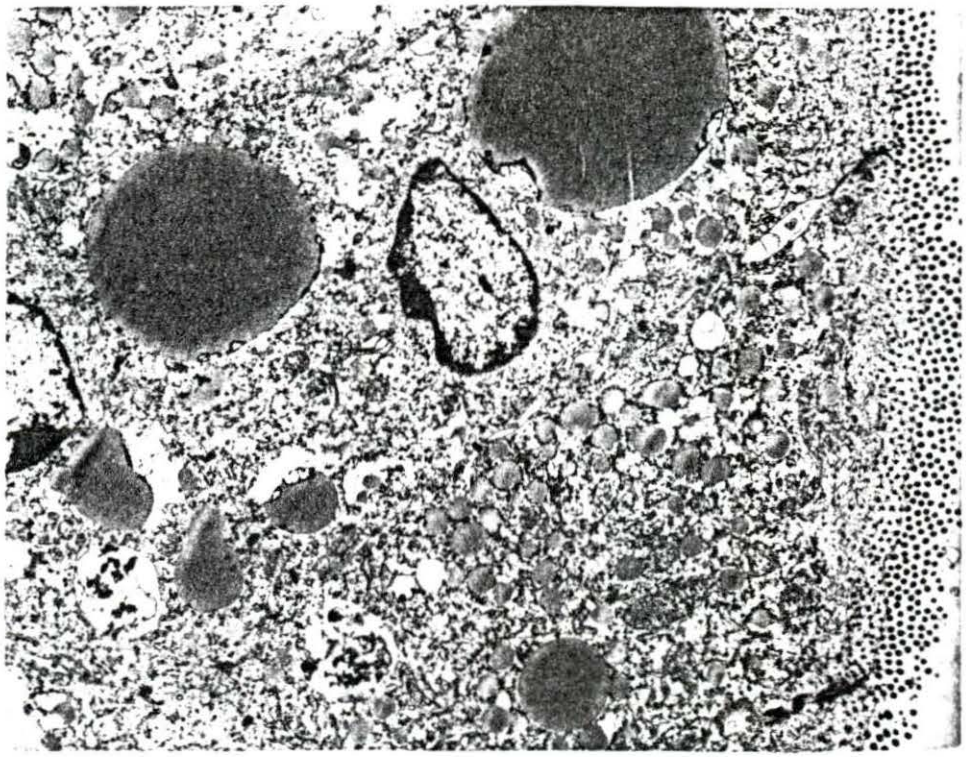

Fig. 15. Crypt cells from an experimentally infected pig. Annulate lamellae are visible (arrow). X 8,600.

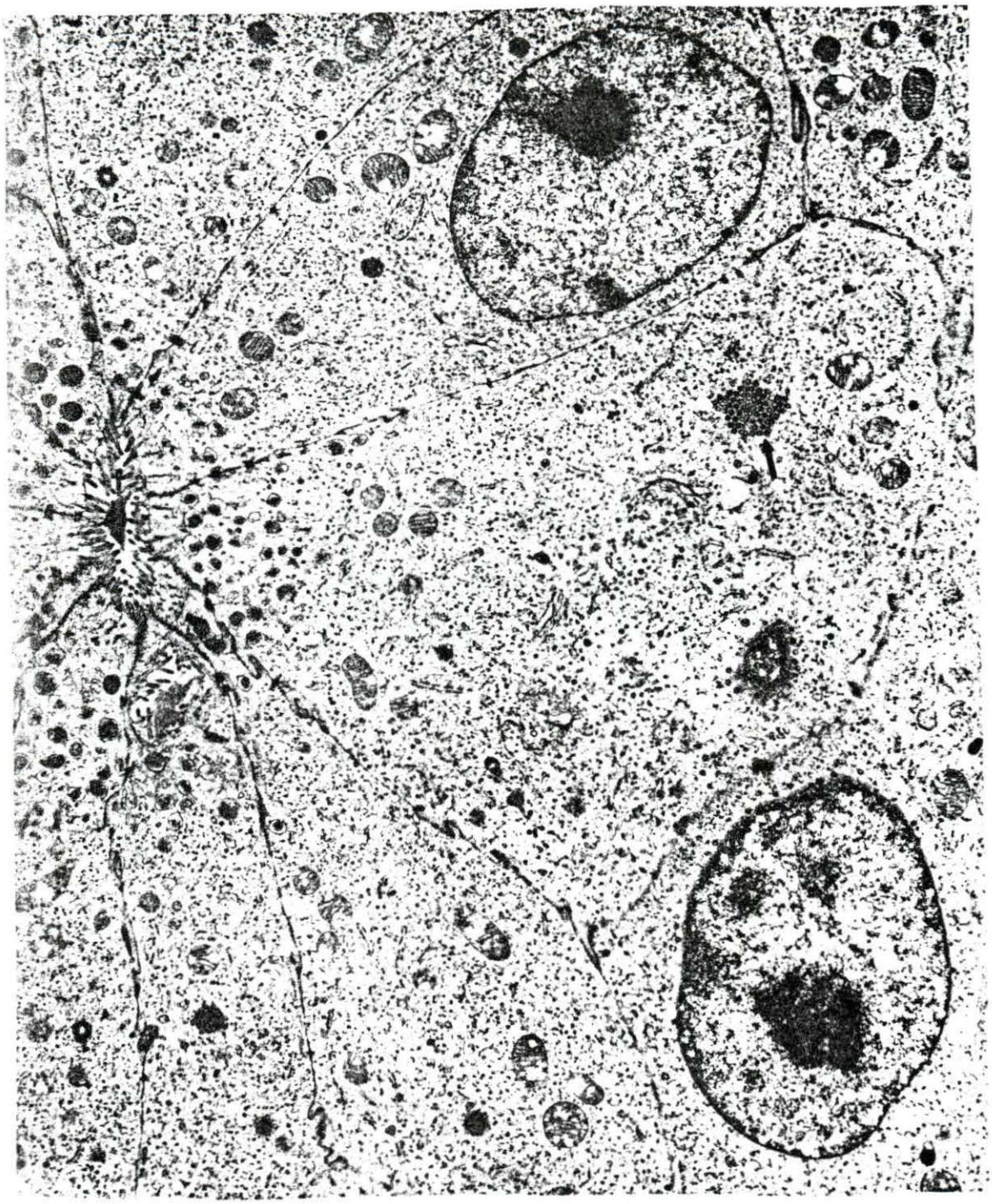

Fig. 16. Villous cells from an experimentally infected pig. The microvillous border is short and irregular. The cytoplasm consists primarily of polyribosomes and contains no pinocytotic vesicles. Vacuoles, containing fine amorphous material, are seen throughout the cytoplasm (arrows) and probably represent sites of extracted fat. X 8,300.

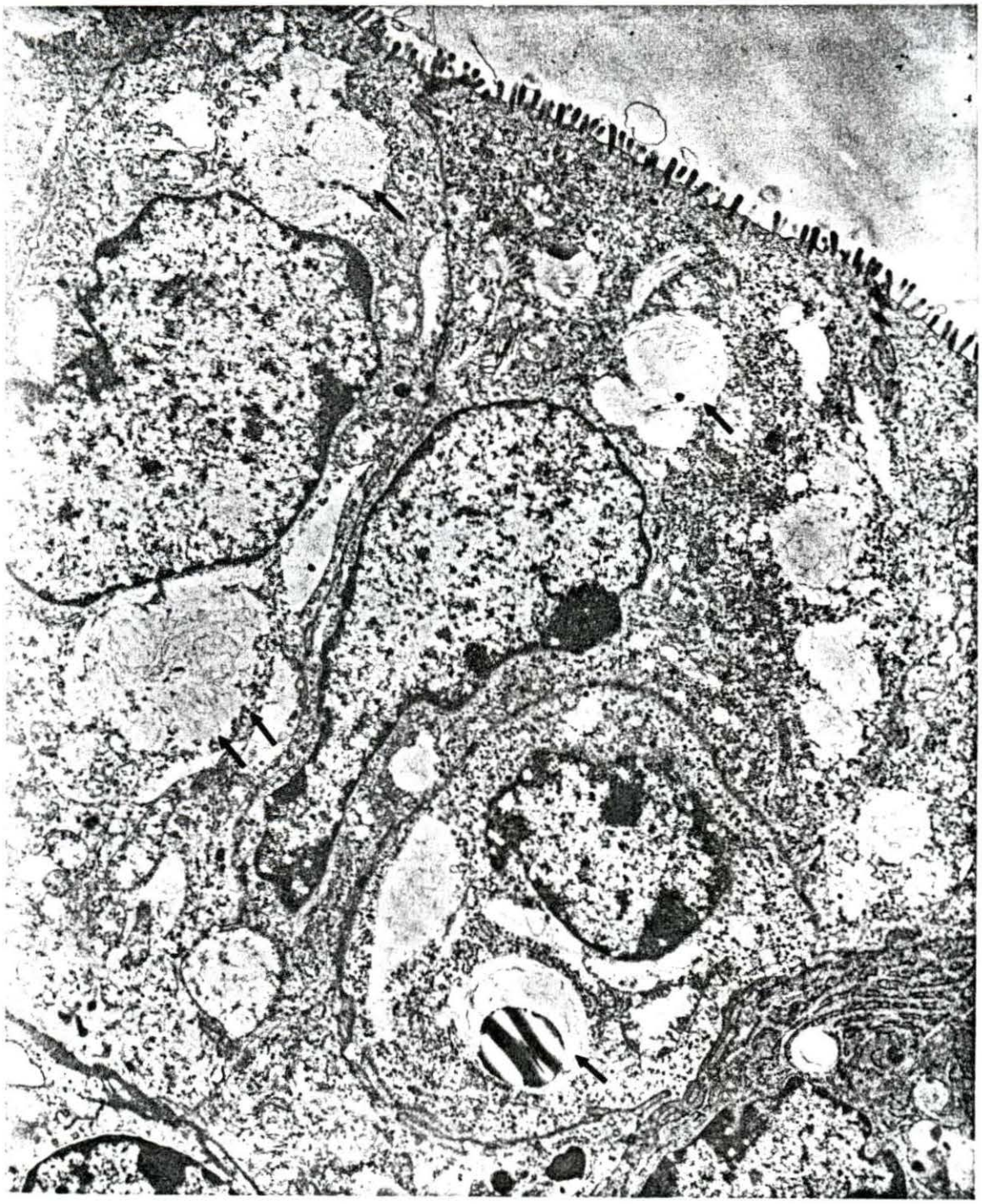

Fig. 17. Villous epithelium from an experimentally infected pig. Excessive accumulations of fat, numerous polyribosomes and absence of pinocytotic vesicles characterize the cells in this section. The microvillous border is only moderately altered in these cells. X 6,700.

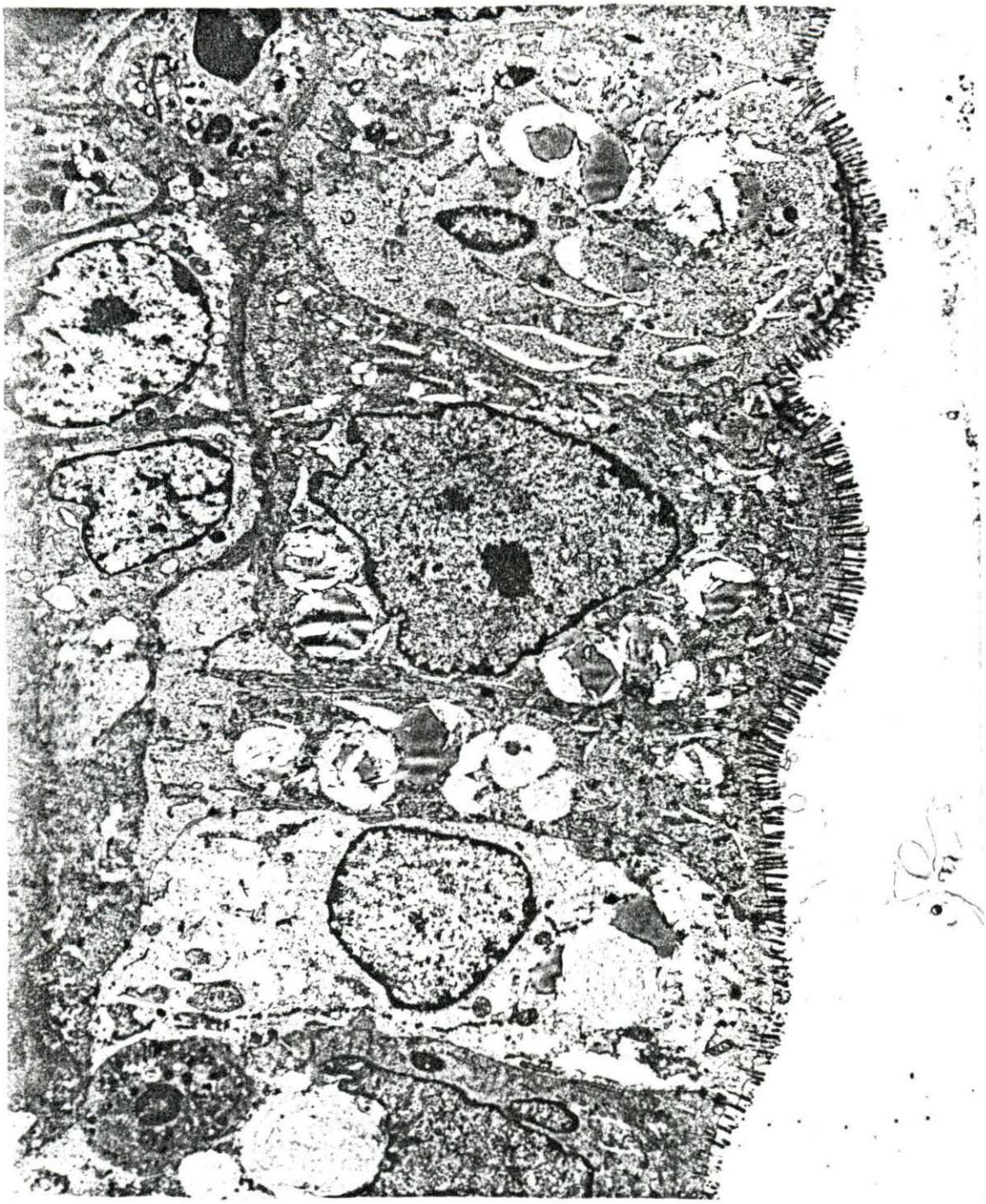

Fig. 18. Cells located near a villous tip in an experimentally-infected pig. The microvillous border is severely affected. A few leukocytes are visible beneath the epithelial cells. X 6,700.

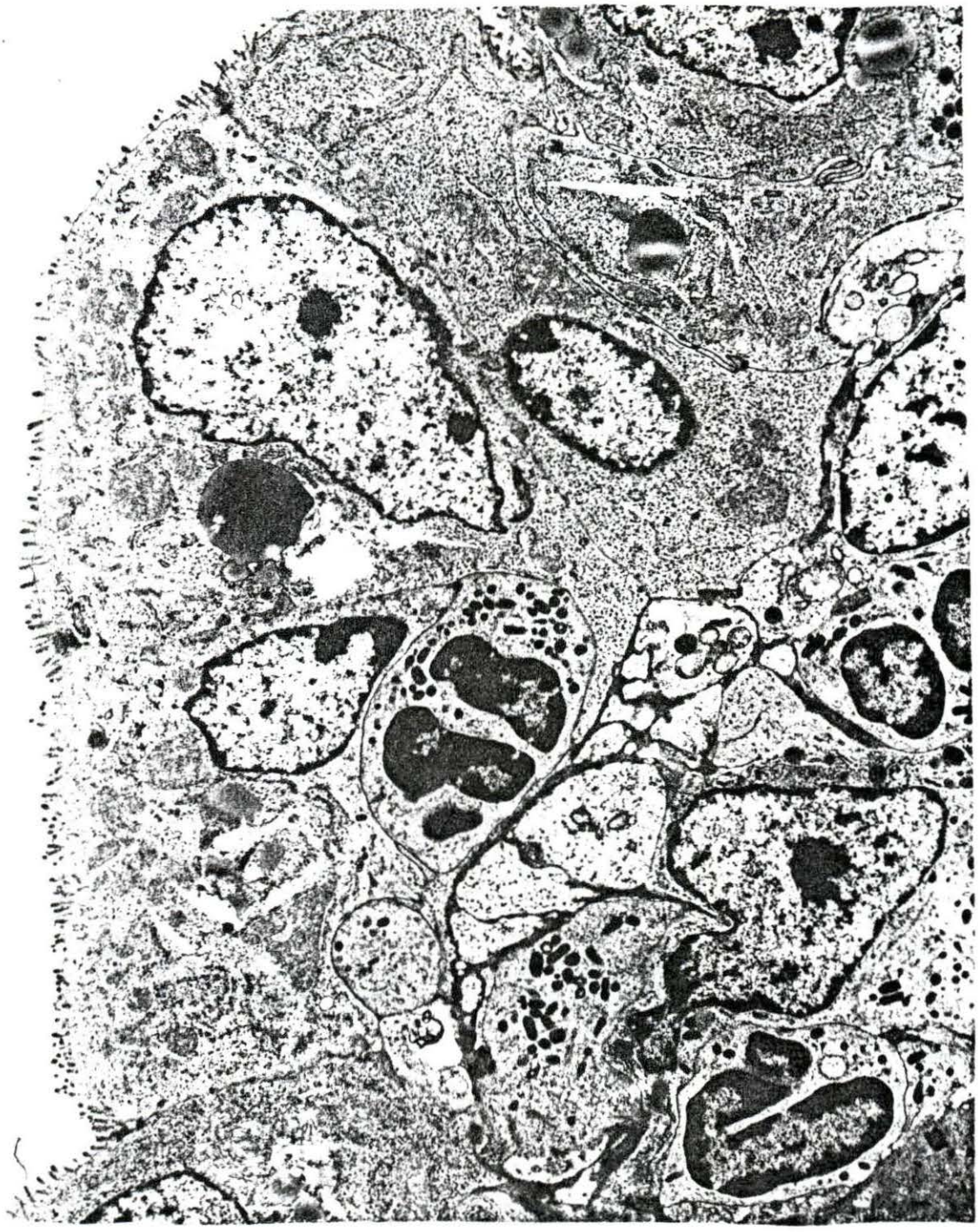

Fig. 19. Annulate lamellae in an epithelial cell of an experimentally-infected animal showing their close association with elements of the granular endoplasmic reticulum. X 17,300.

Fig. 20. Higher magnification of annulate lamellae seen in Fig. 15, showing their structural similarity to nuclear pores. X 27,300.

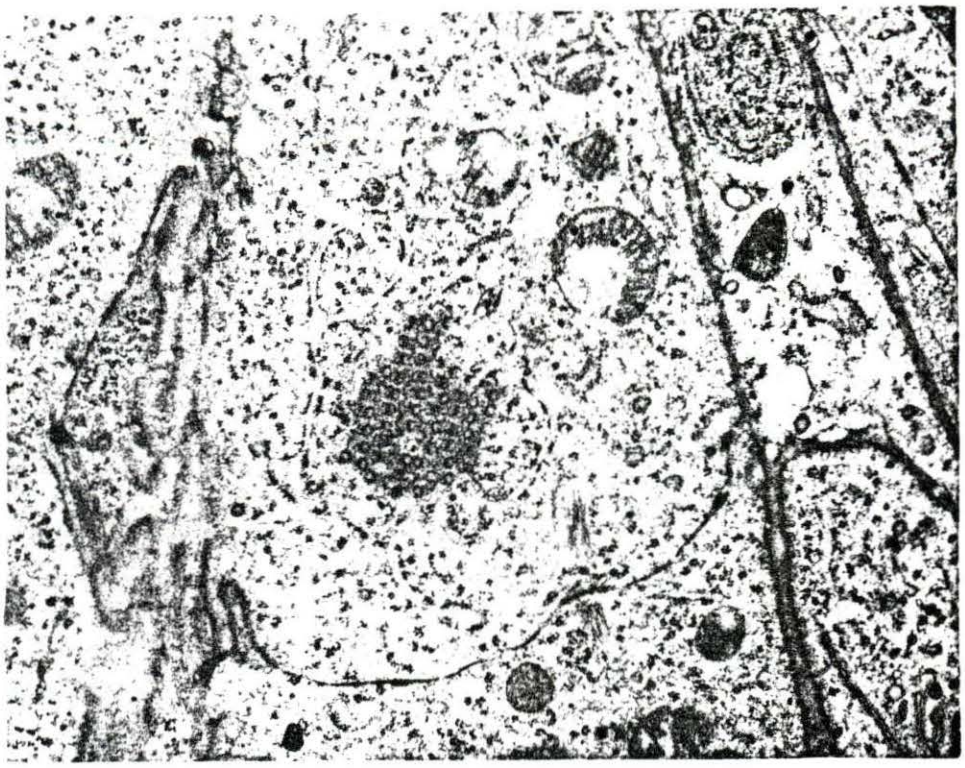

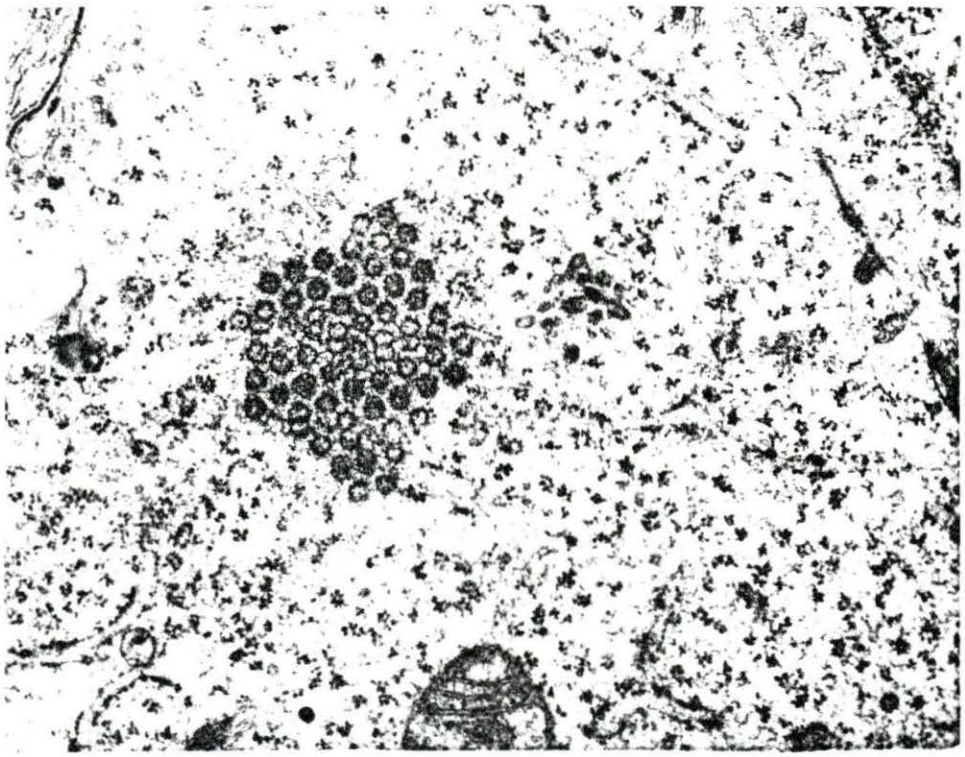

observed in noninfected animals, was most intense in the epithelial cells of the villi (Figs. 22, 24, 26, 28, 30). The crypt epithelium of the pigs at 6 weeks of age stained more intensely for all enzymes than did the crypt cells of the 4-day-old pigs. However, the intensity of the reactions for all enzymes was substantially greater in the villous epithelium, especially toward the villous tips.

Alkaline phosphatase was bilaminar in distribution, being located toward the free surface of the brush border and in the apical cytoplasm just beneath the cell membrane. The crypt cells of the 4-day-old pigs contained only slight amounts of the enzyme, but there was an abrupt increase in intensity of the reaction at the crypt-villous junction (Fig. 22).

Acid phosphatase was most predominant in the apical cytoplasm of the villous cells. The change in reaction intensity was abrupt and occurred at the crypt-villous junction as in alkaline phosphatase (Fig. 24).

Adenosine triphosphatase stained intensely in the villous cells. The localization of this enzyme in crypt cells was greater than that of other enzymes (Fig. 26). There was a more intense staining in the area of the brush border, probably due to nonspecific activity of alkaline phosphatase, since both reactions are carried out at pH 9.4.

Succinic dehydrogenase was present throughout the cytoplasm but seemed to be more concentrated toward the base of the cells. The intensity of reaction for the enzyme increased gradually on the villi, the greatest localization occurring on the surface cells near the tips of the villi (Fig. 28).

Esterase activity was distributed throughout the cytoplasm but appeared slightly more intense in the supranuclear region (Fig. 30). Only minute amounts were present in the crypt cells.

The activity of the 5 enzymes tested was substantially reduced in the villous epithelium of infected animals (Figs. 21, 23, 25, 27, 29). The zone of alkaline phosphatase activity at the apical border of the villous cells was much narrower in the infected pigs (Fig. 21). Adenosine triphosphatase activity was greater in the villous epithelial cells of the infected animals than in crypt cells, but substantially less than in villous epithelium of the noninfected pigs (Fig. 25). The reactions for esterase, acid phosphatase, and succinic dehydrogenase were only slightly greater in the villous epithelium than in the crypt epithelium of infected pigs (Figs. 23, 27, 29). No increase in activity was visible for these 3 enzymes at the zone of maturation. No difference in the staining of the crypt epithelium of control and infected animals was detectable.

Fig. 21. Alkaline phosphatase reaction in an experimentally-infected pig. X 60.

Fig. 22. Alkaline phosphatase reaction in a noninfected control pig. X 150.

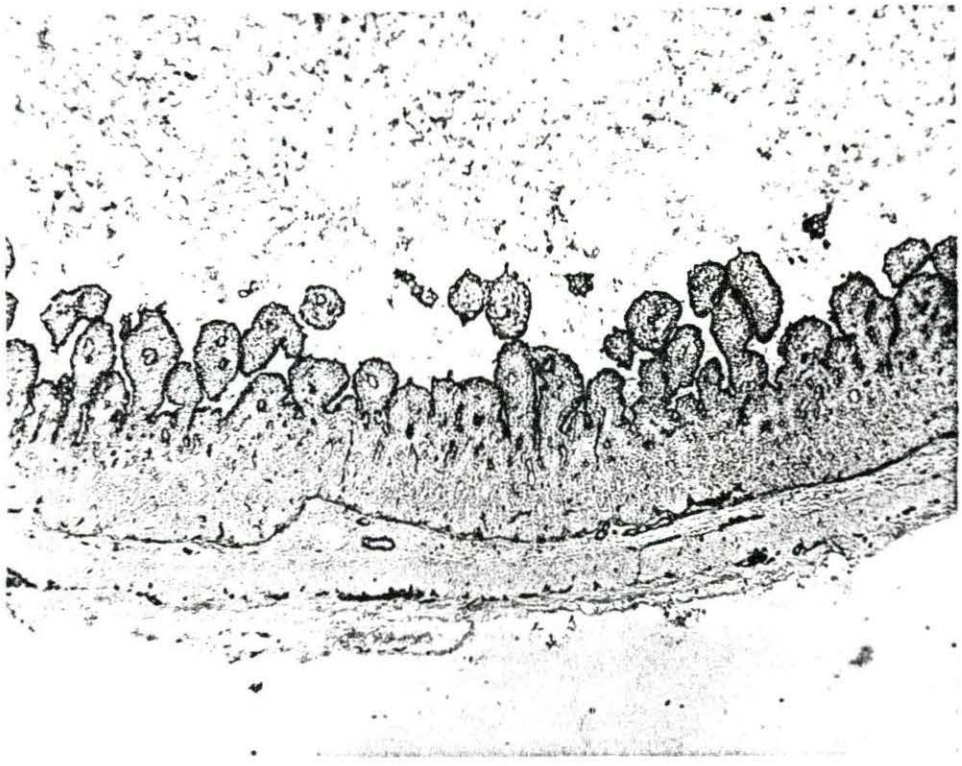

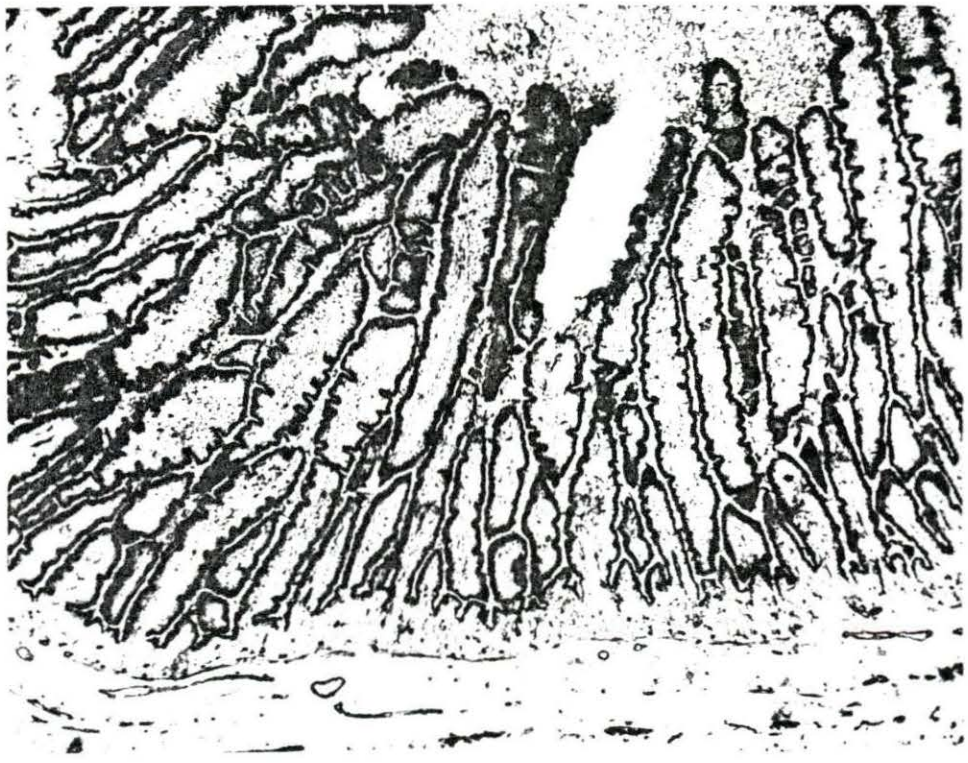

Fig. 23. Acid phosphatase reaction in an experimentally-infected pig. X 150.

Fig. 24. Acid phosphatase reaction in a noninfected control pig. X 150.

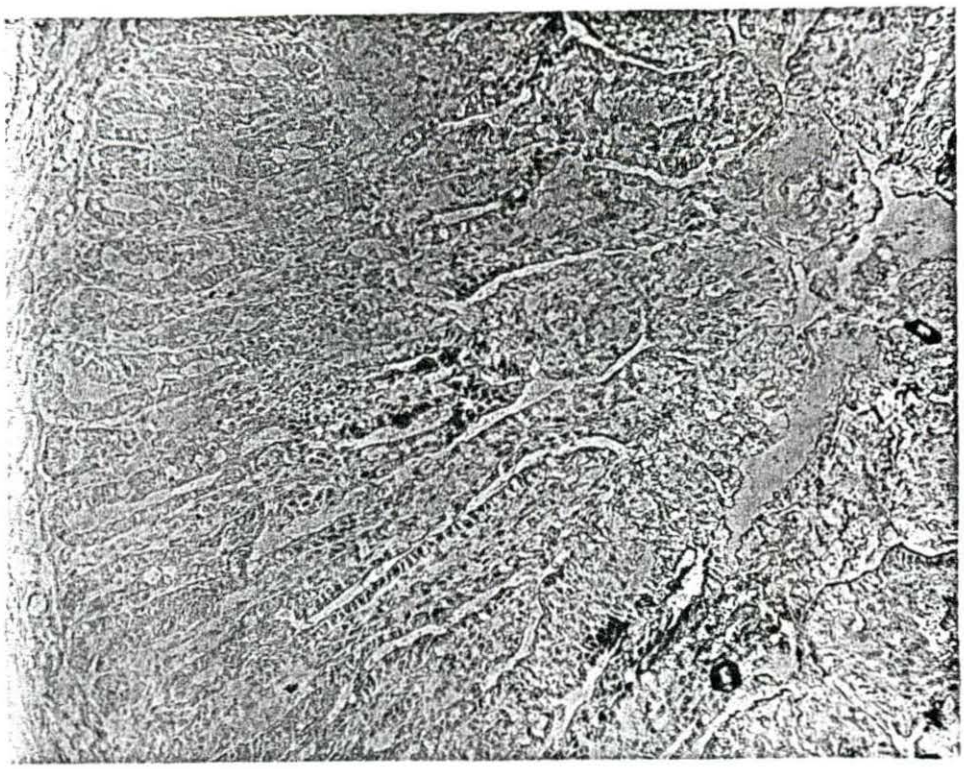

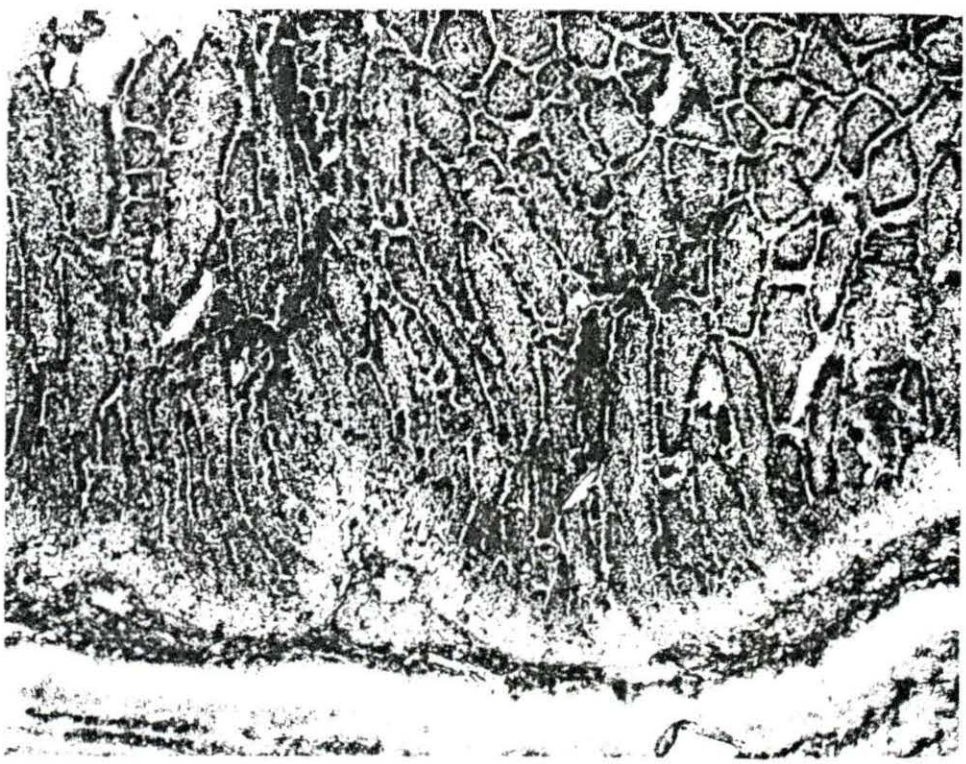

Fig. 25. ATPase localization in an experimentally-infected pig. X 375.

Fig. 26. ATPase localization in a noninfected control pig. X 375.

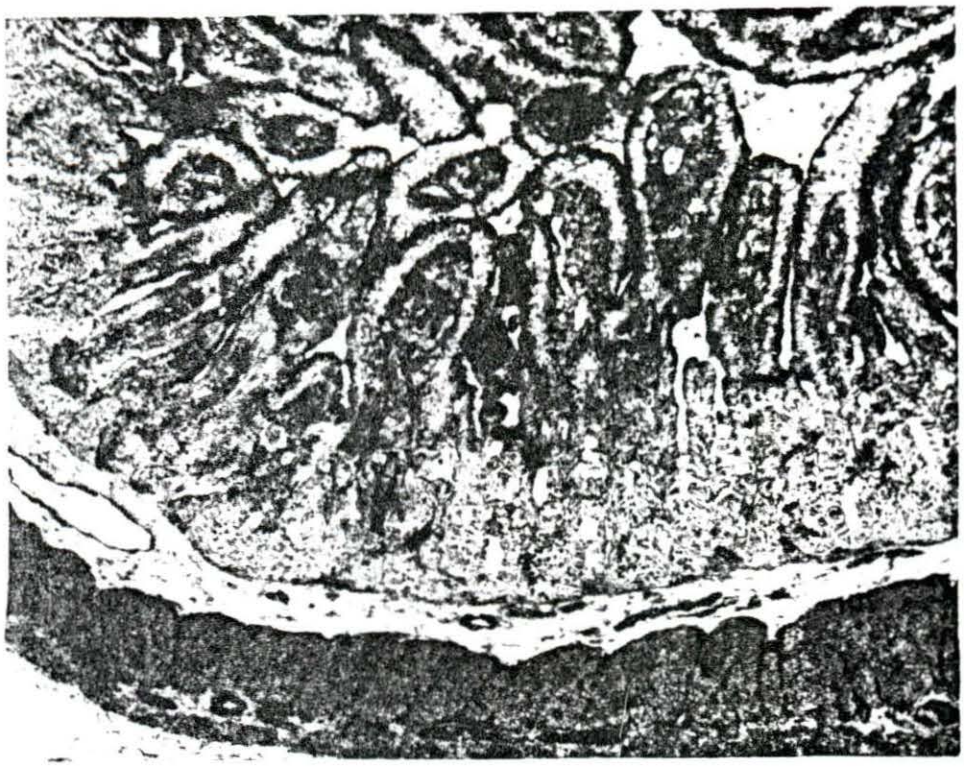

Fig. 27. Succinic dehydrogenase reaction in an experimentally-infected pig. X 150.

Fig. 28. Succinic dehydrogenase reaction in a noninfected control pig. X 375.

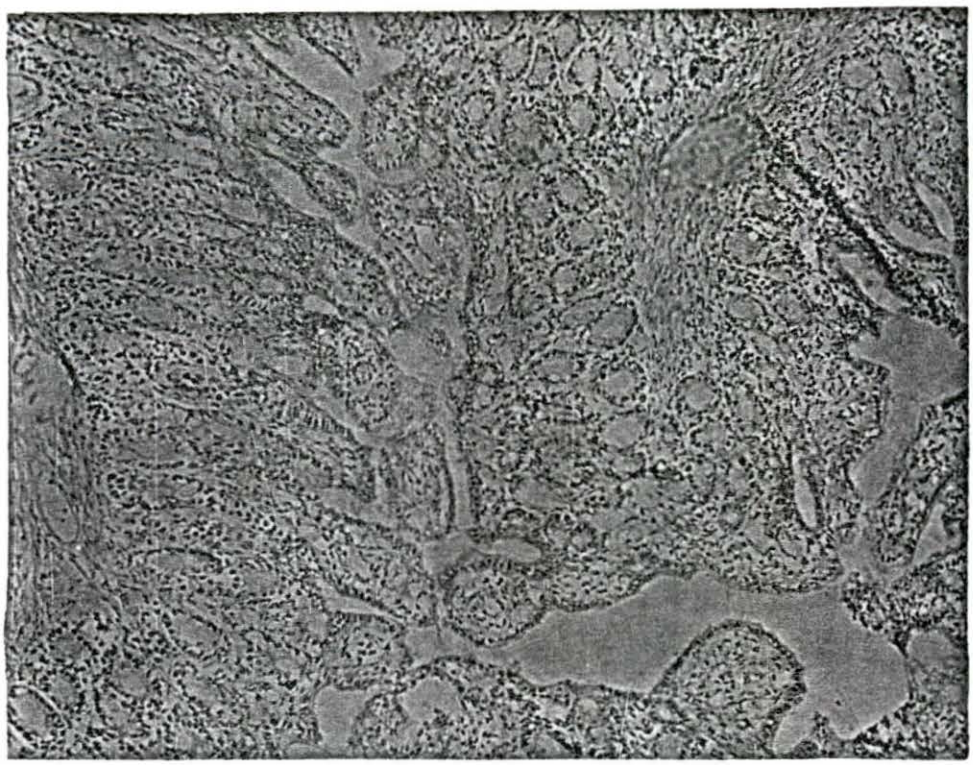

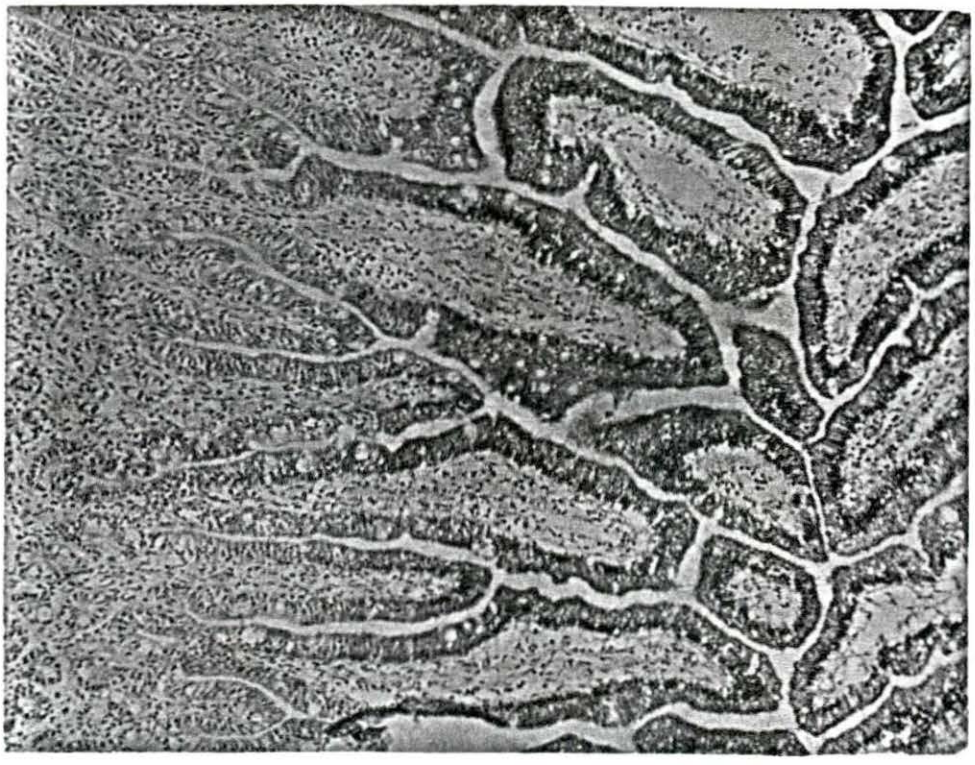

Fig. 29. Nonspecific esterase localization in an experimentally-infected pig. X 600.

Fig. 30. Nonspecific esterase localization in a noninfected control. X 600.

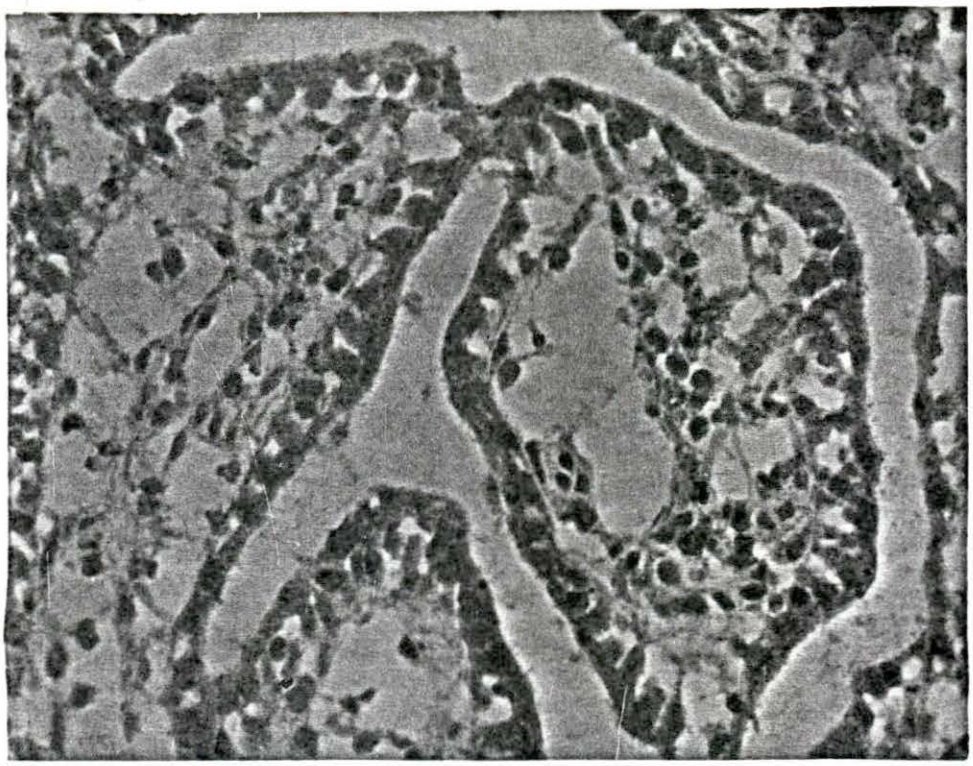

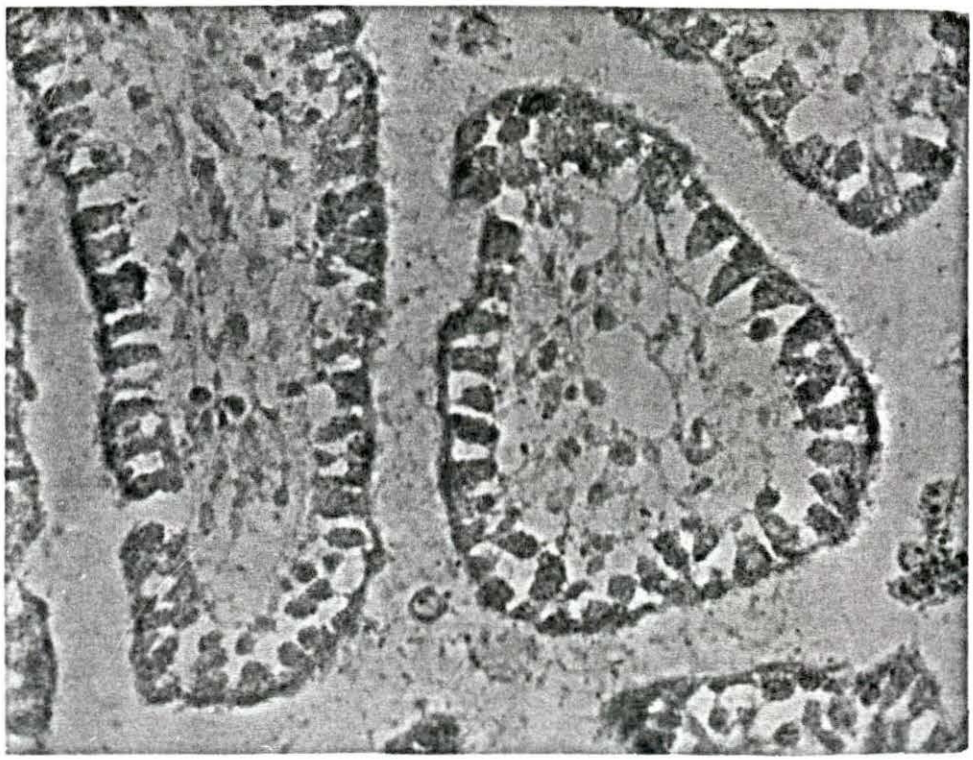

DISCUSSION

Cellular degeneration due to viral replication was evident in villous epithelial cells, with the most extensive changes visible toward the tips of the villi. Cell replication in the crypts was accelerated, probably to compensate for the more rapid destruction of villous cells. This study indicates, however, that normal maturation failed to occur as the cells moved onto the villi. The result was a villous cell population characterized by degenerating and immature cells incapable of normal absorption.

Villous atrophy is the most significant microscopic lesion of TGE (1, 2, 4), although inflammation and denuding of the mucosal epithelium have been reported (7, 9, 10). Villous atrophy occurs also in LIVIM virus infection of infant mice, a disease syndrome which is similar in many respects to TGE in infant pigs (52). Villous atrophy is well known as a lesion of human malabsorption syndromes (41, 53, 54, 55, 56). It can be produced experimentally by the administration of neomycin (57), by irradiation, by substances which inhibit mitosis (37, 38, 58), and it has been reported in salmonellosis in mice (59). The mature cell population of the villi is important in maintaining normal villous structure, for disorders of cell turnover or a reduction in numbers of mature cells results in a compensatory change in the size and shape of the villi (60). Possible mechanisms suggested for villous atrophy are: (1) decreased rate of mitosis with subsequent reduction of epithelial cell numbers (37, 38, 58, 60), (2) arrest in maturation

with decreased epithelial cell migration up the villi (41, 60), (3) excessive rate of cell death and loss of cells from the villous tips (60) and (4) edema and cell infiltration of the lamina propria with adhesions between villi (56, 61).

Mitoses are increased in the intestinal crypts of infected pigs as compared to noninfected controls, even following administration of colchicine to both groups (1), thus eliminating mitotic arrest as the basis for the villous atrophy in TGE-infected pigs. The results of this study suggest that the villous changes in TGE are due to increased cell destruction and improper epithelial cell maturation, resulting in a reduced villous epithelial cell population which is immature and functionally deficient.

Cellular degeneration was evident from electron microscopic observations of the villous epithelium. Mitoses in the crypt cells were increased and the number of cells in the crypt layer was increased. It appeared from this study, however, that the increased mitoses in the crypts were not sufficient to compensate for the increased cell destruction resulting in a diminished mature cell population on the villi. It also appeared that the cells were moving onto the villi while still in an immature state. This was reflected by ultrastructural similarities of the crypt to the villous epithelial cells. The distinctive morphologic features that differentiated villous cells from crypt cells in the control animals were absent in the villous cells of the infected pigs. The abundance of ribosomes, lack of vacuoles and vesicles that result from absorption and the shortened, irregularly arranged microvilli

were the prominent features of normal crypt cells evident in the villous cells of infected animals.

The annulate lamellae seen in both villous and crypt epithelia have been reported previously in a variety of tissues (62, 63, 64, 65, 66, 67, 68, 69, 70). They have been observed in oocytes of invertebrates (65, 68), as well as in the adrenal cortex of fetal rats (69), in the pancreatic acinar cells of rats treated with azaserine (64), in myocardium of chick embryos (67), and in certain neoplastic cells (62, 63). They have also been observed in tissue culture cells (66, 71). The origin and function of these structures are unknown. They appear very closely related to the nuclear membrane, and this has led some to believe they originate from the nuclear membrane. Porter (72) stated that annulate lamellae are prominent in actively growing and multiplying cell populations. Sibalin and Björkman (30) reported stacked lamellae present in jejunal cells of young pigs, but no reference was made to the presence of annuli within these structures. In this study, however, the annular structures were most prominent. These structures were not observed in control animals. The presence of these structures in both crypt and villous epithelium of infected pigs may reflect the undifferentiated state of these cells.

Both villous atrophy and decreased height and numbers of microvilli reduce the amount of absorptive surface area exposed to the lumen of the intestine. However, the significance of microvillous changes must also be viewed in light of their enzyme content. Alkaline phosphatase, amino peptidase, maltase, invertase, lactase, isomaltase and

trehalase are reported to be located primarily within the microvilli (73, 74, 75, 76). The specific location of these enzymes appears to be in the plasma membrane of the microvilli (77, 78). Crane (73, 74) viewed the microvillous border as a digestive-absorptive border, with the terminal digestion of dissacharides and the absorption of the monosaccharides occurring here. Crane (74) also considered primary malabsorption to be caused by the congenital or acquired absence of a specific enzyme-containing protein of the plasma membrane. Secondary malabsorption is considered as that resulting from an over-all reduction in the digestive-absorptive surface secondary to other disease conditions. Hooper (1) found that there is a net reduction in glucose absorption in TGE-infected pigs, which, according to the above concepts, may be directly related to the microvillous changes.

The large fat globules within many of the jejunal epithelial cells may be due to an inability on the part of the cells to transport fat to the lymphatics, such as occurs in puromycin-treated rats, wherein there is apparently an inability to synthesize lipoproteins and form chylomicrons (79). The normal pathway of fat absorption involves movement of the fat into the cell by pinocytosis, after which it becomes incorporated into elements of the granular endoplasmic reticulum and is discharged into the intercellular space at the lateral cell membrane by reverse pinocytosis and subsequently moves to the lymphatics or capillaries of the lamina propria (28). In the infected animals, however, the lateral cell membranes were in close apposition. No intercellular spaces existed, and accordingly no fat was visible in this area. It appeared

that some fat was being absorbed, but that the mechanism for fat transport across the cell was being impaired.

Activity of all 5 enzymes tested was substantially reduced in infected pigs indicating a general reduction of intracellular enzyme content and, consequently, impaired cellular metabolism. Depressed succinic dehydrogenase activity probably reflects an alteration in the biochemical function of the mitochondria or perhaps a decrease in their numbers. The depressed activity of these enzymes would be reflected as a decreased energy-producing capacity of the epithelial cells, which could result in diminished absorption of substances which enter the cell by active transport.

Alkaline phosphatase is localized predominantly in the plasma membrane of the brush border (77, 78). Measurement of alkaline phosphatase activity is a measure of the digestive-absorptive surface (74).

For the purpose of this study, it is important also to consider the cause of the diminished enzymatic activity. All enzymes measured were substantially reduced in the villous cells of the infected pigs. There was little difference in the intensity of the reactions for succinic dehydrogenase esterase and acid phosphatase as the cells moved from the crypts to the villous tips. Failure of the normal development of the intracellular enzyme systems is probably another reflection of their incomplete maturation.

SUMMARY

Morphologic and histochemical characteristics of transmissible gastroenteritis in baby pigs were studied. Results show that the cellular alterations were confined to the villous cells. The ultrastructural and histochemical (enzyme) features of the villous and crypt cells were similar, signifying incomplete villous cell differentiation. Accelerated villous cell destruction resulting from virus replication, together with the improper maturation of the cells, produced villous atrophy and was responsible for the clinical syndrome.

ACKNOWLEDGMENTS

This project was conducted under the United States Government Employees' Training Act Public Law 85507.

The author is indebted to Dr. N. F. Cheville and Dr. J. H. Greve for guidance and assistance during the course of this project.

Photographic assistance by Mr. R. M. Glazier was greatly appreciated.

LITERATURE CITED

1. Hooper, B. E. Transmissible gastroenteritis of swine: studies on the pathogenesis. Microfilm copy, unpublished Ph.D. thesis, Lafayette, Indiana, Library, Purdue University. Ann Arbor, Michigan, University Microfilms, Inc. 1965.

2. Hooper, B. E. and Haelterman, E. O. Concepts of pathogenesis and passive immunity in transmissible gastroenteritis of swine. Am. Vet. Med. Ass'n J. 149: 1580-1586. 1966.

3. Lee, K. M., Moro, M. and Baker, J. A. Transmissible gastroenteritis in pigs. Am. J. Vet. Res. 15: 364-372. 1954.

4. Trapp, A. L., Sanger, V. L. and Stalnaker, E. Lesions of the small intestinal mucosa in transmissible gastroenteritis-infected germ-free pigs. Am. J. Vet. Res. 27: 1695-1702. 1966.

5. Doyle, L. P. and Hutchings, L. M. Transmissible gastroenteritis in pigs. Am. Vet. Med. Ass'n J. 108: 257-259. 1946.

6. Bay, W. W., Hutchings, L. M., Doyle, L. P. and Bunnell, D. E. Transmissible gastroenteritis in baby pigs. Am. Vet. Med. Ass'n J. 115: 245-248. 1949.

7. Feenstra, E. S., Thorp, F., Gray, M. L. and McMillan, W. N. Transmissible gastroenteritis of baby pigs. Am. Vet. Med. Ass'n J. 113: 573-575. 1948.

8. Whitehair, C. K., Grummer, R. H., Phillips, P. H., Bohstedt, G. and McNutt, S. H. Gastroenteritis in pigs. Cornell Vet. 38: 24-28. 1948.

9. Bay, W. W., Doyle, L. P. and Hutchings, L. M. The pathology and symptomatology of transmissible gastroenteritis. Am. J. Vet. Res. 12: 215-218. 1951.

10. Okaniwa, A. and Maeda, M. Histopathology of transmissible gastroenteritis in experimentally infected newborn piglets. Nat. Inst. Anim. Hlth. Quart. 5: 190-201. 1965.

11. Okaniwa, A. and Maeda, M. Histopathology of transmissible gastroenteritis in experimentally infected newborn piglets. II. Lesions in organs other than digestive tract and pathologic feature of TGE. Nat. Inst. Anim. Hlth. Quart. 6: 24-32. 1966.

12. Young, G. A., Hinz, R. W. and Underdahl, N. R. Some characteristics of transmissible gastroenteritis (TGE) in disease free antibody devoid pigs. Am. J. Vet. Res. 16: 529-535. 1955.

13. Reber, E. J. and Whitehair, C. K. The effect of transmissible gastroenteritis on the metabolism of baby pigs. Am. J. Vet. Res. 16: 116-119. 1955.

14. Hooper, B. E. and Haelterman, E. O. Growth of transmissible gastroenteritis virus in young pigs. Am. J. Vet. Res. 27: 286-291. 1966.

15. Haelterman, E. O. Epidemiological studies of transmissible gastroenteritis of swine. U.S. Livestock Sanit. Ass'n Proc. 66: 305-315. 1962.

16. Bay, W. W., Doyle, L. P. and Hutchings, L. M. Some properties of the causative agent of transmissible gastroenteritis in swine. Am. J. Vet. Res. 13: 318-321. 1952.

17. Harada, K., Kumagi, T. and Sasahara, J. Cytopathogenicity of transmissible gastroenteritis virus in pigs. Nat. Inst. Anim. Hlth. Quart. 3: 166-167. 1963.

18. Okaniwa, A., Maeda, M., Haroda, K. and Kaji, T. Electron microscopy of swine transmissible gastroenteritis (TGE) virus in tissue culture cells. Nat. Inst. Anim. Hlth. Quart. 6: 119-120. 1966.

19. Goodwin, R. F. W. and Jennings, A. R. Infectious gastroenteritis of pigs. I. The disease in the field. J. Comp. Path. and Ther. 69: 87-97. 1959.

20. Eto, M., Ichihara, T., Tsunoda, T. and Watanabe, S. Outbreaks of transmissible gastroenteritis among swine in the Kyushu region. Jap. Vet. Med. Ass'n J. 15: 16-20. 1962.

21. Sasahara, J., Harada, K., Hayashi, S. and Watanobe, M. Studies on transmissible gastroenteritis in pigs in Japan. Jap. J. Vet. Sci. 20: 1-6. 1958.

22. Huang, W. T. and Lin, T. C. Outbreaks of transmissible gastroenteritis-like diseases in pigs in Yi San Prefecture (Taiwan). Experimental Report of Taiwan Provincial Veterinary Serum Institute. 1958. Original not available; cited in Haelterman, E. O. Epidemiological studies of transmissible gastroenteritis of swine. U.S. Livestock Sanit. Ass'n Proc. 66: 305. 1962.

23. Vishnaykov, S. I. and Crosheva, C. A. Infectious gastroenteritis in pigs. Veterinaria, Moscow 3: 37-40. 1963. Original not available; cited in Haelterman, E. O. Epidemiological studies of transmissible gastroenteritis of swine. U.S. Livestock Sanit. Ass'n Proc. 66: 305. 1962.

24. Pehl, K. H. and Benndorf, E. Isolation and properties of a filterable agent causing epidemic gastroenteritis among pigs in northern Germany. Arch. Exp. Vet. Med. 14: 953-967. 1960. Original not available; cited in Haelterman, E. O. Epidemiological studies of transmissible gastroenteritis of swine. U.S. Livestock Sanit. Ass'n Proc. 66: 305. 1962.

25. Janowski, H. and Golaszewski, H. Transmissible gastroenteritis of pigs. Med. Vet., Warsaw 17: 281-285. 1961. Original not available; cited in Haelterman, E. O. Epidemiological studies of transmissible gastroenteritis of swine. U.S. Livestock Sanit. Ass'n Proc. 66: 305. 1962.

26. Granger, B. and Baker, R. F. Electron microscope investigation of the striated border of intestinal epithelium. Anat. Record 107: 423-441. 1950.

27. Zetterquist, H. The ultrastructural organization of the columnar absorbing cells of the mouse jejunum. Stockholm, Sweden, Aktiebologet Godvil. 1956.

28. Palay, S. L. and Karlin, L. J. An electron microscopic study of the intestinal villus. II. The pathway of fat absorption. J. Biophys. Biochem. Cytol. 5: 373-384. 1959.

29. Fawcett, D. W. The cell. Philadelphia, Pa., W. B. Saunders Co. 1966.

30. Sibalin, M. and Björkman, N. On the fine structure and absorptive function of the porcine jejunal villi during the early suckling period. Exp. Cell Res. 44: 165-174. 1966.

31. Palade, G. E. A small particulate component of the cytoplasm. J. Biophys. Biochem. Cytol. 1: 59-68. 1955.

32. Trier, J. S. I. The fine structure of the crypt epithelium of the proximal small intestine of fasting humans. J. Cell Biol. 18: 599-620. 1963.

33. Trier, J. S. Studies on small intestinal crypt epithelium. II. Evidence for and mechanisms of secretory activity by undifferentiated crypt cells of the human small intestine. Gastroenterology 47: 480-495. 1964.

34. Leblond, C. P. and Stevens, C. E. The constant renewal of the intestinal epithelia in the albino rat. Anat. Rec. 100: 357-377. 1948.

35. Lipkin, M., Sherlock, P. and Bell, B. Cell proliferation kinetics in the gastrointestinal tract of man. II. Cell renewal in stomach, ileum, colon and rectum. Gastroenterology 45: 721-729. 1963.

36. Quastler, H. and Sherman, F. G. Cell population kinetics in the intestinal epithelium of the mouse. Exp. Cell Res. 17: 420-438. 1959.

37. Williams, A. W. Experimental production of altered jejunal mucosa. J. Path. Bact. 85: 467-472. 1963.

38. Rybak, B. J. Electron microscopic studies of intestinal lesions. I. Aminopterin induced lesions in mice. Gastroenterology 42: 306-318. 1962.

39. Creamer, B. Variations in the small intestinal villous shape and mucosal dynamics. Brit. Med. J. 2: 1371-1373. 1964.

40. Creamer, B. Small intestinal mucosal dynamics and the environment. Brit. Med. J. 2: 1373-1375. 1964.

41. Padykula, H. A., Strauss, E. W., Ladman, A. J. and Gardner, F. H. A morphologic and histochemical analysis of the human jejunal epithelium in nontropical sprue. Gastroenterology 40: 735-764. 1961.

42. Shnitka, T. K. Enzymatic histochemistry of gastrointestinal mucous membrane. Gastroenterology 19: 897-904. 1960.

43. Dawson, I. and Pryse-Davies, J. The distribution of certain enzyme systems in normal human gastrointestinal tract. Gastroenterology 44: 45-60. 1963.

44. Maronpot, R. R. and Whitehair, C. K. Experimental sprue-like small intestinal lesions in pigs. Can. J. Comp. Med. and Vet. Sci. 31: 309-316. 1967.

45. Pearse, A. G. E. Histochemistry; theoretical and applied. 2nd ed. Boston, Mass., Little, Brown and Company. 1961.

46. Padykula, H. A. and Herman, E. Factors affecting the activity of adenosine triphosphatase and other phosphates as measured by histochemical techniques. J. Histochem. 3: 161-169. 1955.

47. Nachlas, M. M., Tsau, K. C., DeSouza, E., Cheng, C. S. and Seligman, A. M. Cytochemical demonstration of succinic dehydrogenase by use of a new p-nitrophenyl substituted ditetrazole. J. Histochem. Cytochem. 5: 420-436. 1957.

48. Bergmeyer, H. U. Methods of enzymatic analysis. New York, N.Y., Academic Press, Inc. 1963.

49. Coons, A. H. and Kaplan, M. H. Localization of antigen in tissue cells. II. Improvements in a method for the detection of antigen by means of fluorescent antibody. J. Exptl. Med. 91: 1-13. 1950.

50. Trautman, A. and Fiebiger, J. Fundamentals of the histology of domestic animals. Ithaca, N.Y., Comstock. 1952.

51. Sloss, M. W. The microscopic anatomy of the digestive tract of Sus scrofa domestica. Am. J. Vet. Res. 15: 578-593. 1954.

52. Biggers, D. C., Kraft, L. M. and Sprintz, H. Lethal intestinal virus infection of mice (LIVIM). Am. J. Path. 45: 413-422. 1964.

53. Rubin, W., Ross, L. L., Sleisenger, M. H. and Weser, E. An electron microscopic study of adult celiac disease. Lab. Invest. 15: 1720-1747. 1966.

54. Curran, R. C. and Creamer, B. Ultrastructural changes in some disorders of the small intestine associated with malabsorption. J. Path. Bact. 86: 1-8. 1963.

55. Padykula, H. A. Recent functional interpretation of intestinal morphology. Fed. Proc. 21: 873-878. 1962.

56. Reid, A. and Brunser, O. Pathogenesis of small intestine changes in celiac disease. Arch. Path. 77: 525-528. 1964.

57. Jacobson, E. D., Prior, J. T. and Faloan, W. W. Malabsorptive syndrome induced by neomycin: morphologic alterations in the jejunal mucosa. J. Lab. and Clin. Med. 56: 245-250. 1960.

58. Clark, P. A. and Harland, W. A. Experimental malabsorption with jejunal atrophy induced by colchicine. Brit. J. Exp. Path. 44: 520-523. 1963.

59. Abrams, G. D., Schneider, H., Formal, S. B. and Sprintz, H. Cellular renewal and mucosal morphology in experimental enteritis: infection with Salmonella typhimurium in the mouse. Lab. Invest. 12: 1241-1248. 1963.

60. Creamer, B. The dynamics of the small intestinal mucosa. In Badenoch, J. and Brooke, B. N., eds. Advances in gastroenterology. Pp. 148-161. Boston, Mass., Little, Brown and Co. 1966.

61. Schenk, E. A., Samloff, M. I. and Klepstein, F. A. Pathogenesis of jejunal mucosal alterations in synechiae formation. Am. J. Path. 50: 523-527. 1967.

62. Chambers, V. C. and Weiser, R. S. An electron microscopic study of Sarcoma I in a homologous host. I. The cells of the growing tumor. Cancer Res. 24: 693-708. 1964.

63. Hoshino, M. Submicroscopic characterization of four strains of Yoshida ascites hepatoma of rats: a comparative study. Cancer Res. 23: 209-216. 1963.

64. Hruban, Z., Swift, H. and Slesers, A. Effect of azaserine on the fine structure of the liver and pancreatic acinar cells. Cancer Res. 25: 708-724. 1965.

65. Kessel, R. G. Intranuclear and cytoplasmic annulate lamellae in tunicate oocytes. J. Cell Biol. 24: 471-487. 1965.

66. Kumegawa, M., Cattoni, M. and Rose, G. G. Electron microscopy of oral cells in vitro. J. Cell Biol. 34: 897-901. 1967.

67. Mercow, Leonard and Leighton, Joseph. Increased numbers of annulate lamellae in myocardium of chick embryos incubated at normal temperatures. J. Cell Biol. 28: 127-137. 1966.

68. Merriam, R. W. The origin and fate of annulate lamellae in maturing sand dollar eggs. J. Biophys. Biochem. Cytology 5: 117-122. 1959.

69. Ross, M. H. Annulate lamellae in adrenal cortex of the fetal rat. J. Ultrastruct. Res. 7: 373-382. 1962.

70. Swift, H. The fine structure of annulate lamellae. J. Biophys. Biochem. Cytol. 2, Suppl. to No. 4: 415-419. 1956.

71. Koestner, A. Kasza, L. and Kindig O. Electron microscopy of tissue cultures infected with porcine polioencephalomyelitis virus. Am. J. Path. 48: 129-147. 1966.

72. Porter, K. R. The ground substance; observations from electron microscopy. In Brachet, Jean and Mirsky, Alfred E., eds. The cell. Vol. 2. Pp. 621-675. New York, New York, Academic Press, Inc. 1961.

73. Crane, R. K. Hypothesis for mechanism of intestinal active transport of sugars. Fed. Proc. 21: 891-895. 1962.

74. Crane, R. K. Enzymes and malabsorption: a concept of brush border membrane disease. Gastroenterology 50: 254-262. 1966.

75. Holt, J. H. and Miller, D. The intestinal border as a digestive surface: localization of aminopeptidase and phosphatase in mucosal epithelial cells (abstract). J. Lab. Clin. Med. 58: 827. 1961.

76. Miller, D. and Crane, R. K. The digestive function of the epithelium of the small intestine. I. An intracellular locus of disaccharide and sugar phosphate hydrolysis. Biochem. et Biophys. Acta 52: 281-293. 1961.

77. Eicholz, A. and Crane, R. K. Studies on the organization of the brush border in intestinal epithelial cells. I. Tris disruption of isolated hamster brush border and density gradient separation of fractions. J. Cell Biol. 26: 687-691. 1965.

78. Overton, J. A., Eicholz, A. and Crane, R. K. Studies on the organization of the brush border in intestinal epithelial cells. II. Fine structure of fractions of tris disrupted hamster brush borders. J. Cell Biol. 26: 693-706. 1965.

79. Sabesin, S. M. and Issebacher, K. J. Protein synthesis inhibition; mechanism of impaired fat absorption. Science 147: 1149-1151. 1965.